iScience

CellPress
OPEN ACCESS

Article

Neuregulin-1/ErbB4 signaling modulates *Plasmodium falciparum* HRP2-induced damage to brain cortical organoids

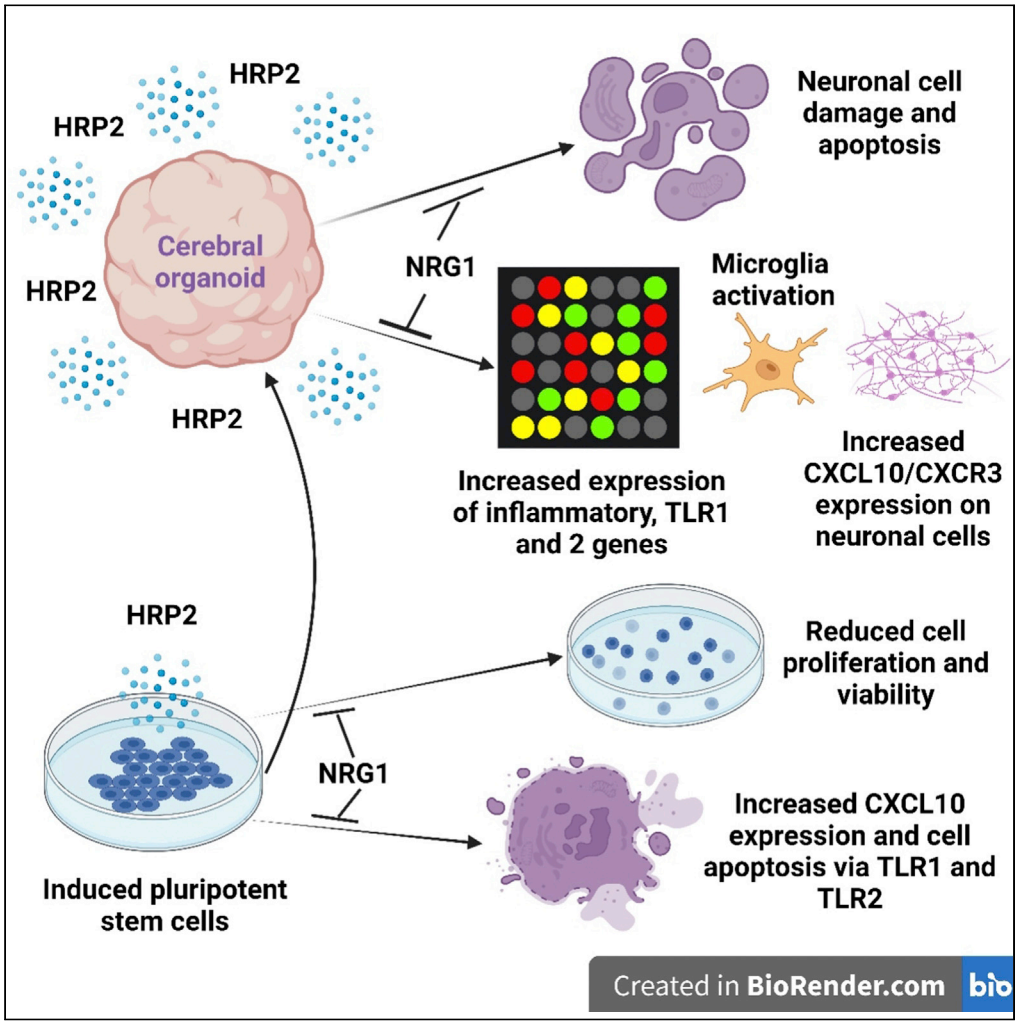

Adriana Harbuzariu, Annette Nti, Keri Oxendine Harp, Juan C. Cespedes, Adel Driss, Jonathan K. Stiles

adriana.harbuzariu@emory.edu (A.H.)
jstiles@msm.edu (J.K.S.)

Highlights

HRP2 induces neuronal injury and microglia activation in cortical organoids

Upregulation of TLR1/TLR2 expression mediates HRP2 effects in brain organoids

NRG1 (100 ng/mL) attenuates HRP2-induced damage via ErbB4 signaling

Harbuzariu et al., iScience *25*, 104407
June 17, 2022 © 2022 The Author(s).
https://doi.org/10.1016/j.isci.2022.104407

iScience

CellPress
OPEN ACCESS

Article

Neuregulin-1/ErbB4 signaling modulates *Plasmodium falciparum* HRP2-induced damage to brain cortical organoids

Adriana Harbuzariu,[1,3,*] Annette Nti,[1] Keri Oxendine Harp,[1] Juan C. Cespedes,[1] Adel Driss,[1] and Jonathan K. Stiles[1,2,*]

SUMMARY

Human cerebral malaria (HCM) is a severe complication of *Plasmodium falciparum (P.f.)* infection that is characterized by capillary occlusions, rupture of the blood-brain barrier (BBB), perivascular cellular injury, and brain swelling. *P.f.*histidine-rich protein 2 (HRP2), a byproduct of parasitized red blood cell (pRBC) lysis, crosses the BBB when compromised to cause brain injury. We hypothesized that HRP2-induced neuronal damage can be attenuated by Neuregulin-1 (NRG1), an anti-inflammatory neuroprotective factor. Using brain cortical organoids, we determined that HRP2 upregulated cell death and inflammatory markers and disorganized brain organoid tissue. We identified toll-like receptors (TLR1 and 2) as potential mediators of HRP2-induced cellular damage and inflammation. Exogenous acute treatment of organoids with NRG1 attenuated HRP2 effects. The results indicate that HRP2 mediates malaria-associated HRP2-induced brain injury and inflammation and that NRG1 may be an effective therapy against HRP2 effects in the brain.

INTRODUCTION

Plasmodium falciparum (P. f.) infections in malaria endemic Sub-Saharan Africa were responsible for 627,000 deaths in 2020, mostly in young children (Bylicka-Szczepanowska and Korzeniewski, 2022). Ninety percent (90%) of fatal cases are associated with HCM, which is characterized by a positive *P.f.* infection, fever, headache, irritability, restlessness, agitation, seizures, vomiting, drowsiness, and rapid-onset of coma in untreated patients (Milner et al., 2014; Phillips and Solomon, 1990). A quarter of surviving children suffer long-term neurological and cognitive deficits including behavioral abnormalities, seizures, and impaired motor function (Bangirana et al., 2016; Fernando et al., 2006). In low endemic settings, all ages are at risk and nonimmune individuals, even at low levels of infection (<1% parasitemia), may develop life threatening HCM (Doolan et al., 2009).

During HCM, parasite destruction of infected erythrocytes results in the release of parasite-derived histidine rich protein 2 (HRP2) and erythrocyte-derived free heme into circulation (Pal et al., 2017; Renia et al., 2012). The circulating cytotoxic free heme mediates oxidative stress, vascular apoptosis, and inflammation (Dutra et al., 2014; Harbuzariu et al., 2019; Soares and Weiss, 2015) in various host tissues including the brain. The elevated levels of HRP2 (a protein that presents histidine in 37% and repeats of histidine and alanine in 85% of its amino acid structure) in the serum of individuals with HCM, which is proportionally higher than levels in uncomplicated malaria patients (Fox et al., 2013; Kariuki et al., 2014), is used to accurately determine presence of circulating parasites and their biomass (Hendriksen et al., 2012; Imwong et al., 2015). HRP2 has been reported to induce inflammatory markers in human brain vascular endothelial cells *in vitro* through an unknown receptor and to reduce the integrity of tight junctions, leading to increased blood brain barrier (BBB) permeability (Pal et al., 2017). As a result, HRP2 reaches the cerebrospinal fluid (CSF) (Mikita et al., 2014) in fatal HCM.

We and others have previously ascertained that Angiopoietin (Ang)-1, Ang-2, CXCL10 (ligand for chemokine receptor CXCR3) (Jain et al., 2011; Lovegrove et al., 2009), brain-derived neurotrophic factor (BDNF) (Cacialli et al., 2018) (McDonald et al., 2017), and Neurofilaments (NF) [light (L)-NFL, medium (M)-NFM, and heavy (H)-NFH] ((Reuterswärd et al., 2018) circulating levels could discriminate between HCM and

[1]Microbiology, Biochemistry and Immunology, Morehouse School of Medicine, Atlanta, GA 30310, USA

[2]Senior author

[3]Lead contact

*Correspondence: adriana.harbuzariu@emory.edu (A.H.), jstiles@msm.edu (J.K.S.)

https://doi.org/10.1016/j.isci.2022.104407

This is an open access article under the CC BY-NC-ND license (http://creativecommons.org/licenses/by-nc-nd/4.0/).

uncomplicated malaria, correlate with coma recovery, and predict severity of HCM clinical outcome. In postmortem CSF samples, the levels of IL-1ra, IL-8, CXCL10, MIP-1β, sFas, Fas-Ligand, sTNF-R1, and sTNF-R2 were significantly higher in children with HCM compared with children who died of non-malaria-related causes (Armah et al., 2007), suggesting that brain cells are exposed to and/or secrete these inflammatory factors. Although *in vitro* exposure of human brain vascular endothelial cells (HBVEC) and neuroglia to pRBC soluble factors induced apoptosis (Wilson et al., 2008), neuroglia appeared to be less susceptible than HBVEC and the mechanisms mediating the cellular damage were unknown.

Recent efforts to identify adjunctive therapeutics against HCM-associated brain injury and sequelae yielded NRG1 that functions through a receptor tyrosine protein kinase (ErbB4) and is widely known to play an important role in normal brain cortical development (Flames et al., 2004; Lopez-Bendito et al., 2006; Yau et al., 2003). In the adult brain, NRG1 and ErbB4 are widely expressed and control synaptic plasticity (Chen et al., 2010; Petryshen et al., 2005). NRG1 inhibits lipopolysaccharide-induced Interleukin (IL)-6 and Tumor Necrosis Factor (TNF)-α release and controls Nuclear factor kappa-light chain enhancer of activated B cell (NF-kB) signaling in microglial cells (Simmons et al., 2016). We have reported previously that NRG1 protects against microvascular endothelial and neuronal cell apoptosis, while its circulating levels declined with malaria severity (Liu et al., 2018). Moreover, infusion of NRG1 reduced systemic and brain pro-inflammatory factors (TNFα, IL6, IL1α, and CXCL10) and increased anti-inflammatory factors IL-5 and IL-13 in a murine experimental cerebral malaria (ECM) model (Solomon et al., 2014).

HCM non-survivor brain samples have extremely limited availability and only provide cross sectional analysis, impairing assessment of longitudinal malarial effects. *In vitro* and experimental mice models of cerebral malaria (ECM) have also yielded limited success in modeling the human disease (murine model does not support cytoadhesion and lacks PfEMP1 proteins). Primate *Plasmodium* infection showed pathological changes similar to those of human HCM, especially because they sequester parasitized erythrocytes (pRBC) and develop petechial hemorrhages in brain parenchyma (de Souza and Riley, 2002). Despite the suitability of these models for investigating malaria pathogenesis, there are human-specific characteristics of brain development, including cortical expansion, which differ in other animal models, and therefore lead to misinterpretation of data and potential failure of new therapies in clinical trials (Zhao and Bhattacharyya, 2018). To overcome the limitations of existing disease models, we were the first group to specifically utilize iPSC-derived brain organoids to demonstrate heme-induced cellular apoptosis and inflammation associated with HCM pathogenesis (Harbuzariu et al., 2019). In this study, we used Cluster of Differentiation (CD)34+-derived iPSC to demonstrate that HRP2 treatment alters cell proliferation and viability, whereas NRG1 exhibits neuroprotective effects through an ErbB4-mediated pathway. Furthermore, we used iPSCs to generate cortical organoids that recapitulate some important aspects of the human brain development (cytoarchitecture, cellular composition, and function) to investigate the direct effects of *P.f.*-derived HRP2 on the human brain.

RESULTS

NRG1 attenuates HRP2 inhibition of iPSC proliferation

The persistence of circulating HRP2 in the plasma of HCM patients even after parasite clearance led to investigations into its functional role during malaria pathogenesis. For example, a study using radiolabeled HRP2 investigated its specific binding to T and B cells and found that it was specific, concentration dependent, saturable, and reversible and that HRP2 suppressed lymphocyte proliferation (Das et al., 2006). To ensure consistency and reproducibility in our studies, the iPSCs (Figure S1) were authenticated based on colonies morphology (smooth edges and tightly packed cells with high nuclear: cytoplasm ratio) and their phenotype (Sox2+, Oct-4+, and SSEA4+). Then, we determined the amount of HRP2 necessary to reduce iPSC proliferation by >30% to be 4.2 μg/mL (Figure S2). We considered this dose to be appropriate for use in our experiments, because a study in Malawi showed that a circulatory HRP2 level of 3500 ng/mL was the cutoff above which clinical deterioration and progression to HCM occurred (Fox et al., 2013). Moreover, another study in Tanzania showed that fatal cases of HCM were associated with HRP2 circulating levels of 4000 ng/mL (Rubach et al., 2012). We treated iPSC's with 4.2 μg/mL L-histidine, Poly L-histidine (HRP2 negative controls), HRP2 alone or in combination with 100 ng/mL NRG1 after 8 h of HRP2 treatment (Figure 1A and S3) and showed that while L-histidine and Poly L-histidine did not change iPSC proliferation/pluripotency, HRP2 significantly reduced iPSC growth and altered their pluripotency markers expression. The addition of NRG1 exogenous treatment significantly increased iPSC proliferation by 40%. HRP2-mediated inhibition of iPSC proliferation occurred over several hours and peaked after 8 h (compared to six or 10

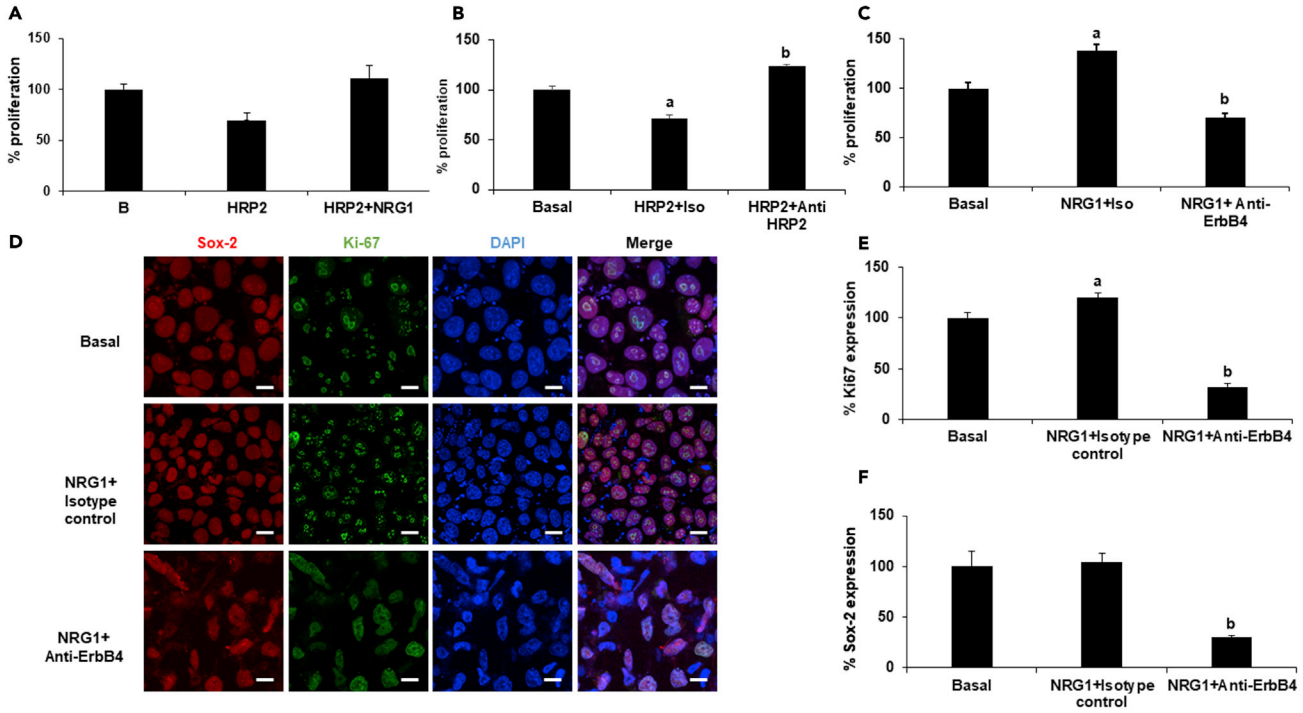

Figure 1. HRP2 inhibition of iPSC proliferation is attenuated by NRG1

(A) Quantification of iPSC growth after HRP2 treatment shows a significant decrease in iPSC proliferation, whereas NRG1 attenuates this effect (B) Addition of monoclonal anti-HRP2 antibody blocks HRP2 effects, whereas isotype control has no effect.

(C) Treatment with monoclonal anti-ErbB4 antibody reduces NRG1-induced iPSC proliferation suggesting that NRG1 effects are ErbB4 signaling-dependent (D) Representative monolayered iPSC cultures incubated with NRG1 and isotype control/anti-ErbB4 antibody and stained for Ki67 for proliferation and Sox-2 for pluripotency (E), (F) Ki67 is increased and Sox2 expression is not significantly changed in iPSC treated with NRG1, whereas anti-ErbB4 antibody attenuates NRG1 effects. Data are represented as mean ± SEM of at least 3 replicates per treatment from 3 separate experiments. a: $p < 0.05$ compared to basal; b: $p < 0.05$ compared to HRP2 treatment. One-way ANOVA or *t*-test were used. Scale bar: 20 μm.

h, Figure S2). Antibody blockade of HRP2 abolished this effect (Figure 1B). NRG1-mediated proliferative effects occurred via ErbB4-mediated signaling, because the antibody blockade of this receptor abrogated NRG1 cytoprotection (Figure 1C). Although some cellular apoptotic bodies could be observed in all conditions (Figure 1D), we confirmed that NRG1 induces iPSC proliferation (Ki-67 expression-Figure 1E) and maintains their pluripotency (Sox-2 expression-Figure 1F).

HRP2 induces structural damage and apoptosis in iPSC-derived cortical organoids

Brain cortical organoids were developed from iPSC and characterized. Our protocol generates highly homogenous cortical organoid cultures with stratified neuroepithelial loops that express the forebrain marker, forkhead box G1 (Foxg1) (Harbuzariu et al., 2019) and the neural stem cell marker, Sox2 at 20 days in culture. Our present studies show that with time, the organoids are further differentiated into more complex and organized structures and are composed of a ventricular (VZ) and subventricular zone (SVZ), as well as a cortical plate (as marked by dashed line). After 50 days in culture, besides Sox-2 positive neuronal stem cells, we began to identify abundant neuron-specific class III β-tubulin (TUJ1) positive mature neurons and cells positive for classical microglial marker ionized calcium binding adaptor molecule 1 (IBA-1) throughout the organoid structure. The IBA1+ fraction within the organoids showed limited variation between batches. Interestingly, extremely few double-positive Brachyury and IBA1+ cells are still observed in our organoids (white arrow) at day 50 in culture, suggesting that mesodermal Brachyury + cells convert to microglia IBA1+ cells in our model as previously described (Ormel et al., 2018). To further characterize the temporal patterning of cortical organoids, cells with astrocyte morphology were detected at approximately 100 days in culture, as found in other studies (Renner et al., 2017) (Figure 2A). Therefore, our results show that some of the brain organization can be recapitulated *in vitro* by our cortical organoids that can be used to model HRP2-induced cellular injury.

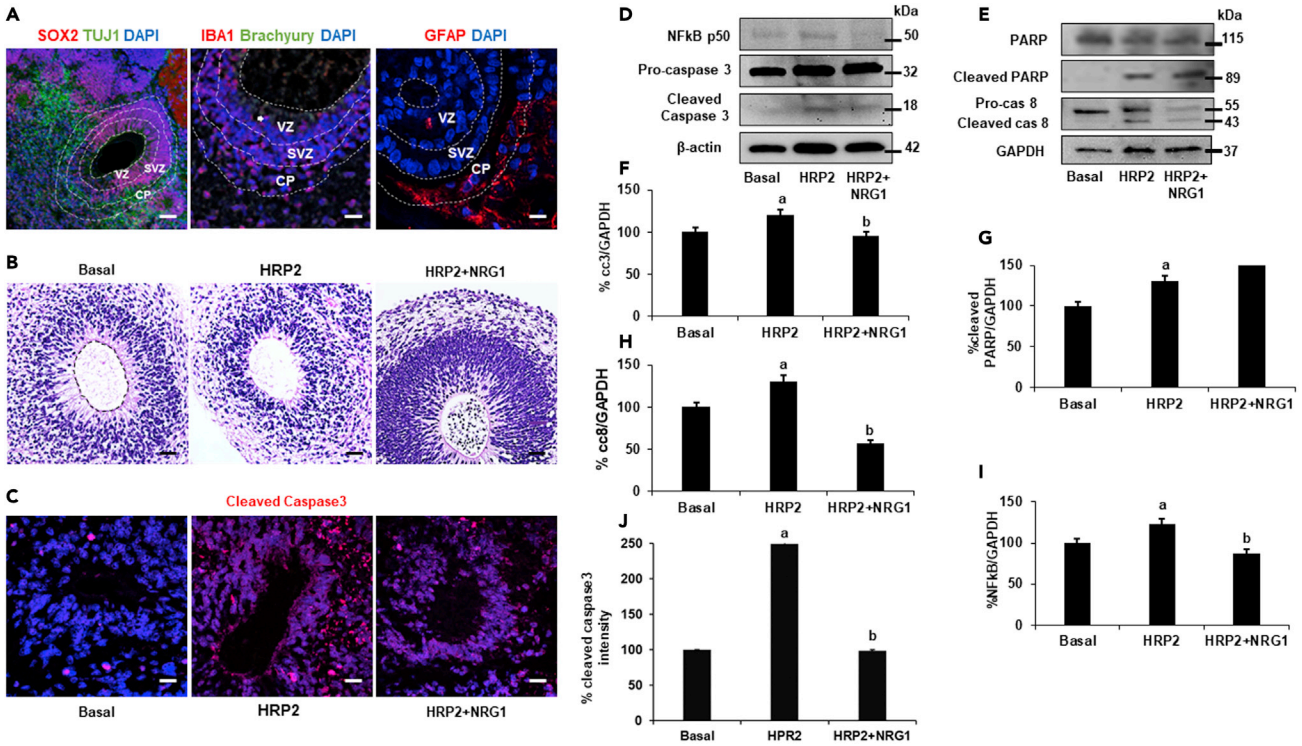

Figure 2. HRP2 induces structural damage and apoptosis in iPSC-derived cortical organoids

(A) Representative z stack projections of paraffin-embedded cortical organoids sections show the expression of neuronal stem cells (Sox-2), mature neurons (TUJ1), and mesoderm-derived microglia (IBA-1 and very few Brachyury) at 50 days in culture, as well as astrocytes (GFAP) at 100 days in culture. After cortical organoids were treated with HRP2 for 8 h, NRG1 was added for 18 h, (B) HRP2 induced disorganization of cortical structures. (C, J) Representative images and quantification of cleaved caspase three expression showed that it increased throughout the organoid structure when HRP2 was added, whereas NRG1 decreased this effect. (D,E) Western blot densitometry of cell lysates treated with HRP2 and NRG1 confirms that HRP2 induces cell death through a caspase 3/caspase 8/PARP-mediated pathway (F-H) and that NFkB expression increased (I). Data are represented as mean ± SEM ImageJ software was used to quantify protein expression (IHC and WB) from at least 3 organoids in 3 experiments. (a: $p < 0.05$ compared to basal conditions; b: $p < 0.05$ compared to HRP2 treatment; One-way ANOVA or *t*-test were used). Scale bar: 20 μm.

P. falciparum parasite-derived HRP2 has been reported to disrupt the integrity of BBB *in vitro* (Tripathi et al., 2007). Using an established human cerebral microvascular endothelial cell line (hCMEC/D3) (Cruz-Orengo et al., 2014; Daniels et al., 2013), we and others have determined that adding heme or parasitized erythrocytes (pRBC) to the upper chamber of a *trans* well plate decreased the endothelial electrical resistance (Pal et al., 2016) and disrupted barrier integrity (Liu et al., 2018). We have previously demonstrated that heme, a by-product of erythrocyte hemolysis during malaria pathogenesis, disrupted the VZ and SVZ where neuronal stem cells reside and the intermediate zone. Hematoxylin and eosin (H&E) staining of 50 days old cortical organoids treated with HRP2 showed disorganized organoid structures in the proximity of the ventricle area (black arrows), whereas NRG1 treatment repaired the damage (Figure 2B). Representative images of red fluorescence showing cleaved caspase 3 (CC3) expression in 40 days old organoids demonstrated that HRP2 significantly increased apoptosis (by 249.3% compared to untreated), whereas NRG1 addition to HRP2 reduced these effects to the basal levels (Figures 2C and 2J). Western blot (Figures 2D and 2E) confirmed that the CC3 expression changed the trend observed for HRP2 and NRG1 treatments (Figure 2F). Furthermore, HRP2 increased cleaved caspase eight and cleaved Poly (ADP-ribose) Polymerase (PARP) (Figures 2G and 2H), while NFkB is activated because of inflammation in organoid tissue (Figure 2I). These results show that HRP2 induces apoptosis in cortical organoids through a caspase 3/PARP/caspase eight mediated pathway, whereas NRG1 attenuates these effects.

HRP2 damages neuronal cells and activates microglia in cortical organoids

Postmortem studies describe areas of fibrinogen extravasation, ring hemorrhage, and ruptured capillaries in the brain of HCM children. In the areas of vascular damage, myelin loss and axonal damage were increased, suggesting that blood-derived factors contributed to parenchymal damage (Dorovini-Zis

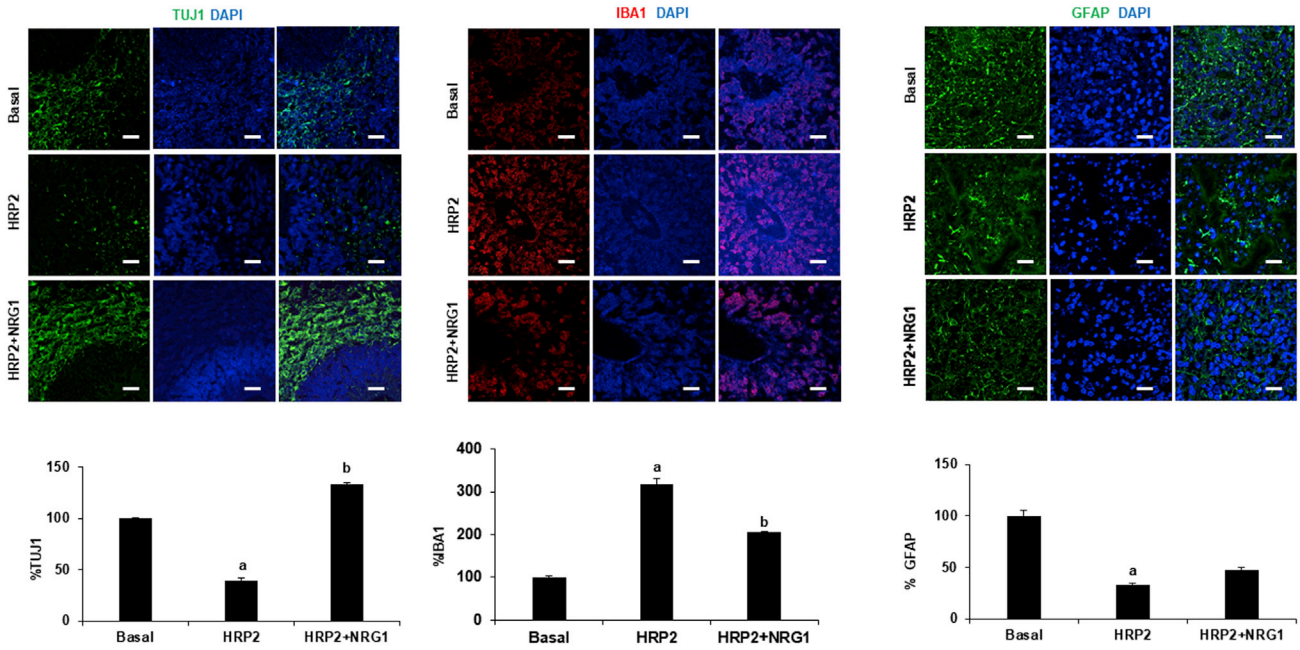

Figure 3. HRP2 damages neuronal cells and activates microglia in cortical organoids

Representative images of brain organoids treated with HRP2 for 8 h, then supplemented with NRG1 for 18 h, and stained for TUJ1 for neurons, IBA1 for microglia, and GFAP for astrocytes. Quantification of TUJ1 and GFAP expression indicate that neurons and astrocytes are injured compared to untreated control, while microglia is activated, leading to inflammation. The addition of NRG1 ameliorated these effects. Data are represented as mean ± SEM of at least three replicates per treatment from 3 separate experiments. a: $p < 0.05$ compared to basal conditions; b: $p < 0.05$ compared to HRP2 treatment. One-way ANOVA and *t*-test were used. Scale bar: 20 μm.

et al., 2011). HCM patients with pRBC sequestration and microvascular pathology demonstrated increased brain gliosis (Medana et al., 2002). Increased BBB permeability during ECM and HCM allows free heme, cytokines, and malaria parasite-derived antigens to enter the brain compartment where they are normally excluded, leading to cellular damage (Hunt et al., 2006). To investigate which cell type is affected the most by HRP2 treatments, we stained 50-day-old cortical organoids for TUJ1 (neurons), IBA1(microglia), and 100 days organoids for Glial Fibrillary Acidic Protein (GFAP) (astrocytes). The results show that HRP2-induced inflammation leads to microglial activation (IBA1 expression increased to 316.7%) and neuronal/astrocyte injury (TUJ1 decreased to 39.7% and GFAP to 32.9%) (Figure 3), suggesting that astrocytes could be more susceptible to HRP2-induced damage.

HRP2 increases neuronal injury marker BDNF and decreases Neurofilaments-medium expression in cortical organoids

To determine whether HRP2 alters the NRG1/ErbB4 axis that is functionally active during brain injury, we showed that HRP2 (4.2 ng/mL) and heme (38 μM) (Harbuzariu et al., 2019), elevated the expression of endogenous NRG1 and decreased ErbB4. However, the addition of exogenous NRG1 (100 ng/mL) to the organoids medium reversed these effects. These results confirm the findings in HCM postmortem brain cortex samples, where the expression of NRG1 increased compared to postmortem brain samples from patients that did not have malaria infection (data not shown). Furthermore, our results show that expression of BDNF, a marker of neuronal injury, is elevated by HRP2 (Figures 4A and 4B). Neurofilaments, structural scaffolding proteins, are increasingly used as specific neuronal injury biomarkers in neurodegenerative, inflammatory, and traumatic diseases in CSF and serum. For example, immunohistochemistry (IHC) of human brain tissue after stroke showed increased NFL at the border of the infarct zone, whereas NFM and NFH expression was reduced (Mages et al., 2018). Our results demonstrate that while NFM was significantly decreased by HRP2 to 39.6%, its expression was slightly increased by NRG1 (Figures 4E and 4F). Although NFL expression was not significantly changed, there was an increasing trend observed with HRP2 (Figures 4C and 4D) and a decreasing trend with heme treatments. Interestingly, unlike HRP2, heme treatment does not change the expression of NFM (Figure S4), suggesting that it could be used not only as a neuronal but also as a HRP2-specific marker of injury in HCM.

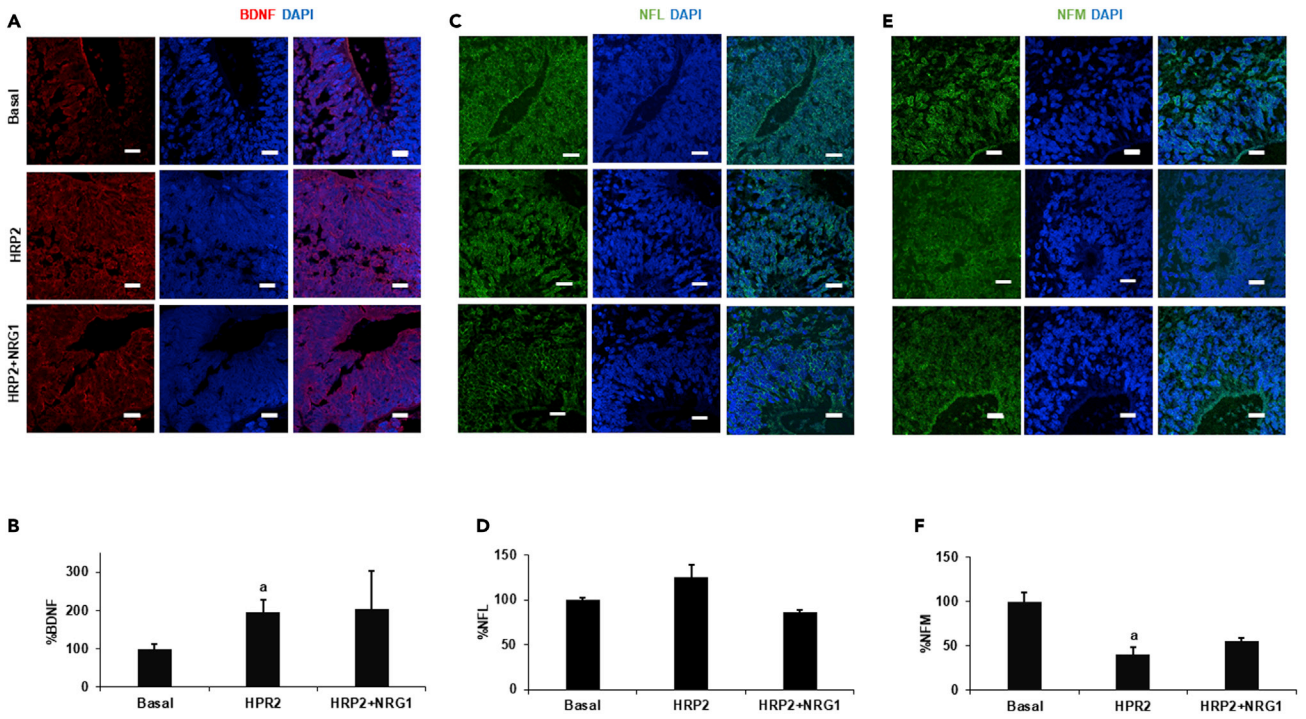

Figure 4. HRP2 increases the expression of neuronal injury markers BDNF and reduces Neurofilaments-medium in cortical organoids

Representative cortical organoids sections treated with HRP2 and NRG1 and stained for BDNF (at the age of 20 days) (A) and Neurofilaments-Large (NFL) (C) and Neurofilaments–Medium (NFM (at the age of 50 days) (E). Quantification of at least three organoids from 3 separate experiments (B) shows that BDNF expression increased compared to untreated controls, whereas NFL remained unchanged (D) and NFM decreased (F). Data are represented by means ± SEM of at least three replicates per treatment from 3 separate experiments. a: $p < 0.05$ compared to basal conditions; b: $p < 0.05$ compared to HRP2 treatment. T test and One-way ANOVA was used. Scale bar: 20 μm. Please also see Figure S2.

HRP2 induces inflammatory cytokines (CXCL10, Ang2/Ang1 ratio) in cortical organoids

Our previous studies demonstrated that increased circulating levels of the pro-inflammatory chemokine, CXCL10, exacerbates pathogenesis of severe malaria in Ghanaian children (Armah et al., 2007). We have recently reported that cellular expression of CXCL10 is increased in cortical organoids when exposed to heme (Harbuzariu et al., 2019). IHC of postmortem HCM brain samples showed that microscopic hemorrhages were associated with increased Ang2 and decreased Ang1 expression compared to non-infected controls (Prapansilp et al., 2013). To assess the HRP2 pro-inflammatory effects, we treated 50-day cortical organoids with 4.2 μg/mL HRP2 for 8 h and then with 100 ng/mL NRG1 for 18 h (Figure 5). The results demonstrate that HRP2 increased CXCL10 expression by 22.1% and its receptor by 32.6% compared to control, whereas NRG1 reduced this effect to a level that was lower than untreated (Figures 5A–5D). Moreover, HRP2 decreased Ang1 expression by 23% compared to untreated (Figures 5E and 5F), whereas Ang2 increased by 52.1% (Figures 5G and 5H). These results suggest that Ang2: Ang1 ratio is increased by HRP2, mimicking observations in HCM, which qualifies it to be a marker for HRP2-induced inflammation. Furthermore, NRG1 treatment decreased the Ang2: Ang1 ratio to baseline levels.

HRP2 increases pro-inflammatory and Toll-like receptor (TLR) genes in cortical organoids

To assess inflammatory genes induced by HRP2, we used the Immunology Panel on the nCounter system (NanoString), and results were analyzed using nSolver software. We treated 50-day cortical organoids (n = 3) for 26 h with 4.2 μg/mL HRP2, whereas untreated samples (n = 3) were used as control. Total RNA was extracted and used to perform the nCounter assay. Genes with a fold-change of at least 1.5 were used to generate a heatmap (Figure 6A). Out of the HRP2-induced genes, most participated in fetal (19.1%) or cortical (29.8%) development and in dendritic cells (23.4%) or monocytes (25.5%) function (Figure 6B). Furthermore, we determined that HRP2-induced genes were mostly involved in the ErbB4 receptor signaling network (46.7%), binding on chemokines to their receptor signaling (12%) and endogenous TLR signaling (12%) (Figure 6C). Using FunRich pathway analysis software, we investigated the genes

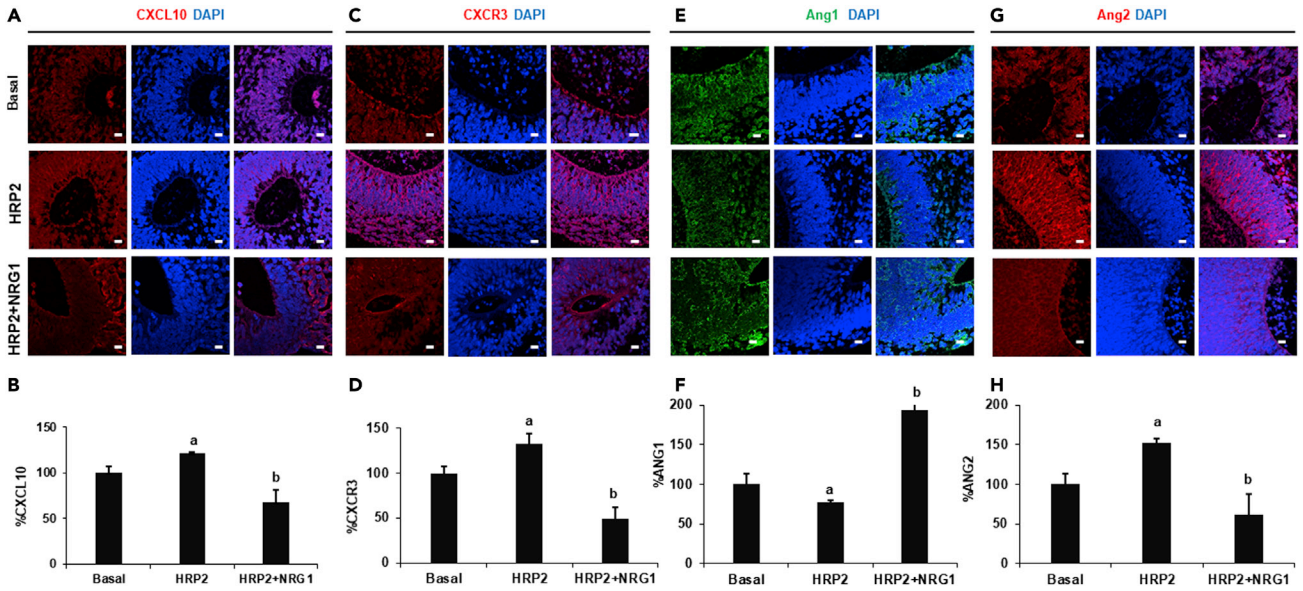

Figure 5. HRP2 induces inflammatory cytokines (CXCL10, Ang2/Ang1 ratio) in cortical organoids

Representative cortical organoids at 50 days in culture treated with HRP2 and NRG1 and stained for CXCL10 (A), its receptor CXCR3 (C), Angiopoietin 1 (E), and Angiopoietin 2 (G). Quantification of CXCL10 (B), CXCR3 (D), Ang1 (F), and Ang2 (H) shows that HRP2 significantly induces inflammation. CXCL10, CXCR3, and Ang2 are increased by HRP2, whereas NRG1 reversed this effect. Data are represented as means ± SEM of N = 3 biological replicates; a: $p < 0.05$ compared to basal conditions; b: $p < 0.05$ compared to HRP2 treatment. One-way ANOVA and *t*-test were used. Scale bar: 20 μm.

associated with the TLR2 pathway and demonstrated that the pathway was modulated by HRP2 (Figure 6D). We determined that TLR1 and TLR2 proteins were induced in a similar manner by HRP2, as shown by densitometry analysis of the western blot bands (Figure 6E and 6F), which was confirmed by IHC for TLR2 (Figure S5A). Furthermore, we showed that in organoids treated with HRP2, the number of microglia (IBA1+) cells expressing TLR2 increased, confirming once again that HRP2 pro-inflammatory effects are TLR2-dependent (Figure S5B).

HRP2 upregulates CXCL10 expression and cell death in iPSC via TLR1 and TLR2

To demonstrate the specific HRP2 pro-inflammatory and proapoptotic effects on iPSCs, we compared the expression of cleaved caspase 3 and CXCL10 in iPSCs treated with HRP2 and its negative controls (L-histidine and Poly L-histidine). Although the random histidine-containing proteins did not influence iPSC viability, there was a trend to increase CXCL10 expression, but the changes were not significant compared to untreated conditions. However, HRP2 significantly increased iPSC apoptosis and expression of CXCL10 compared to untreated controls (Figure S6). Previous studies have demonstrated that TLR2 activates parasite recognition and induces rapid activation of innate immunity by triggering the production of pro-inflammatory cytokines (Campos et al., 2001). To determine whether TLR1 and TLR2 function as receptors for HRP2, we functionally blocked TLR1 and TLR2 using monoclonal antibodies for 1 h before 24 h of HRP2 treatment. Results showed that TLR1/2 blockage only partially restored iPSC proliferation (Figure 7A) in HRP2-treated iPSC, whereas their apoptosis and necrosis (Figures 7B and 7C) reduced control levels. The effects of TLR1 and TLR2 blockage on HRP2-treated iPSC viability was confirmed by immunohistochemistry (Figures 7D and 7F), where the expression of cleaved caspase 3 was reduced. Moreover, the expression of pro-inflammatory CXCL10 was reduced by TLR blockage in HRP2-treated iPSCs (Figures 7E and 7G).

DISCUSSION

Histidine Rich Protein 2 (HRP2), secreted by *P.f.*, is not only used as a biomarker for rapid parasite diagnosis [RDT (Poti et al., 2020)] but also plays an important role in HCM pathogenesis. Children are more likely than adults to remain RDT (HRP2) positive for up to 61 days after antimalarial treatment (Dalrymple et al., 2018). Interestingly, the recent emergence of HRP2-deficient malaria parasites in parts of Africa, South America, and Southeast Asia may account not only for the rising false-negative rates of HRP2 RDTs but also for the

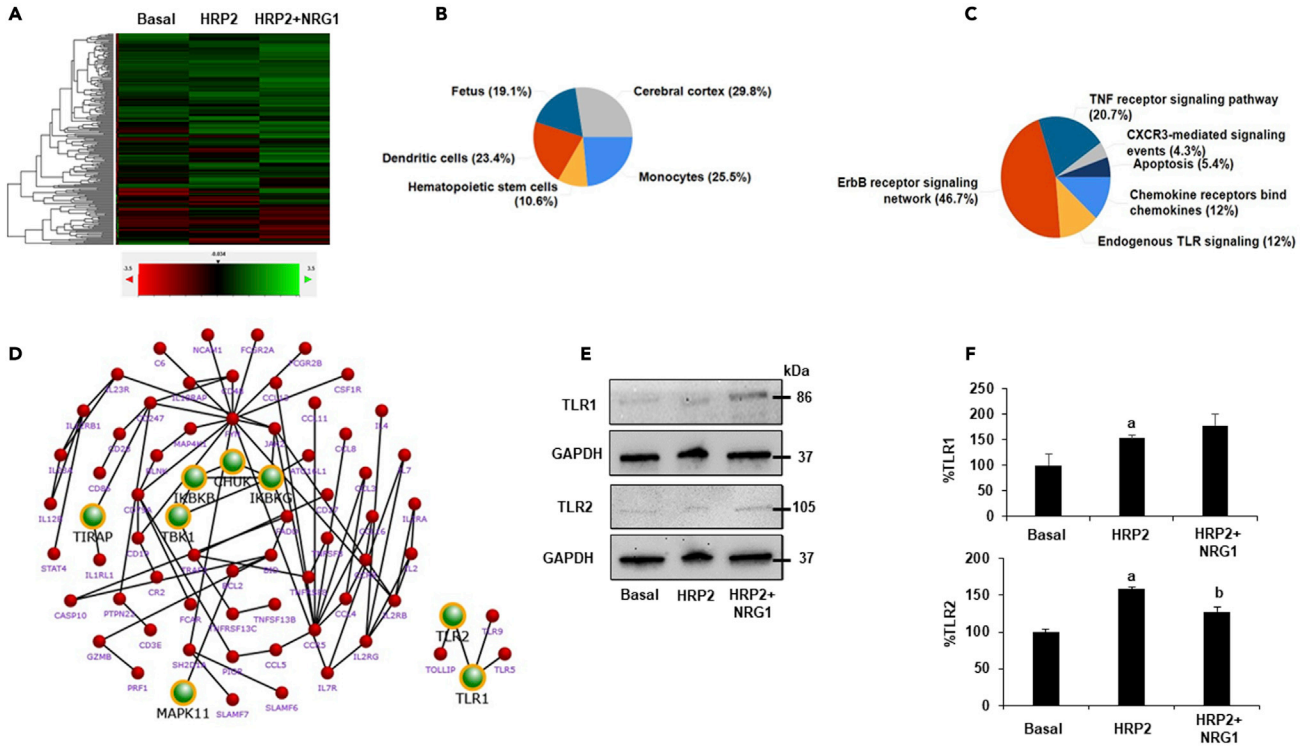

Figure 6. HRP2 increases pro-inflammatory and Toll-like receptor (TLR) genes in cortical organoids. HRP2-induced inflammation-related genes were profiled

Fold changes greater than 1.5 and p values < 0.05 calculated using Student's *t*-test was considered to be a significant dysregulation. (A) A heatmap was generated showing up-and down-regulated genes. The effects of HRP2 on cortical organoids at day 50 in culture are shown by site (B), including cerebral cortex and glia, as well as by pathway (C), including TLR signaling. Further analysis revealed the relationship between upregulated genes and activation of TLR2 pathway (D). Western blot densitometry of organoid lysates (data represented as means ± SEM) confirms that HRP2 significantly induces TLR2 and TLR1 expression, whereas NRG1 reduces these effects (E, F). a: $p < 0.05$ compared to basal conditions; b: $p < 0.05$ compared to HRP2 treatment. One-way ANOVA and *t*-test were used. Please also see Figure S4.

declining rates of severe HCM and HCM mortalities in these regions (Pal et al., 2017). Further field investigations are required to ascertain the validity of this assertion.

HRP2 induces the expression of cytoadherence molecules on endothelial cell surface, promoting adherence, and suppressing the proliferation of B and T lymphocytes, contributing to parasite evasion of the host immune system (Das et al., 2006). Intravenous infusion of recombinant HRP2 in an ECM model induced vascular leakage in the cortices and increased mortality (Pal et al., 2016). HCM survivors, especially children, may present lifelong neurological sequelae [seizures, loss of speech, hearing deficits, behavioral problems, and neurocognitive deficits (Idro et al., 2010)] that affect their quality of life, suggesting that extensive brain neuronal injury may occur. Studies have shown that axonal damage and demyelination, associated with microglial response, occur in the areas of petechial hemorrhages in HCM (Medana et al., 2002). Our previous study determined that the increased expression of IL-1β and TNF is not only perivascular but also is present in the brain parenchyma of postmortem HCM patients and was highest in the cortical area (Armah et al., 2005). Since then, we have determined that CXCL10 increases in postmortem cortical sections of HCM patients compared to non-malaria controls (data not shown). The extensive neuroinflammation and neuronal damage associated with HCM driven by brain apoptosis and/or inflammation may be counteracted by the overall robustness of heme scavenging, immunity to malaria, and tissue repair in the host. These factors may depend on host genetics and susceptibility and may explain why a subset of HCM cases survive and recover or present neurological sequelae, whereas others die regardless of appropriate treatments.

Previous studies have shown that cleaved caspase three expression increased in HCM postmortem cerebrum sections (Punsawad et al., 2013) and have been confirmed by our group (data not shown). Because human

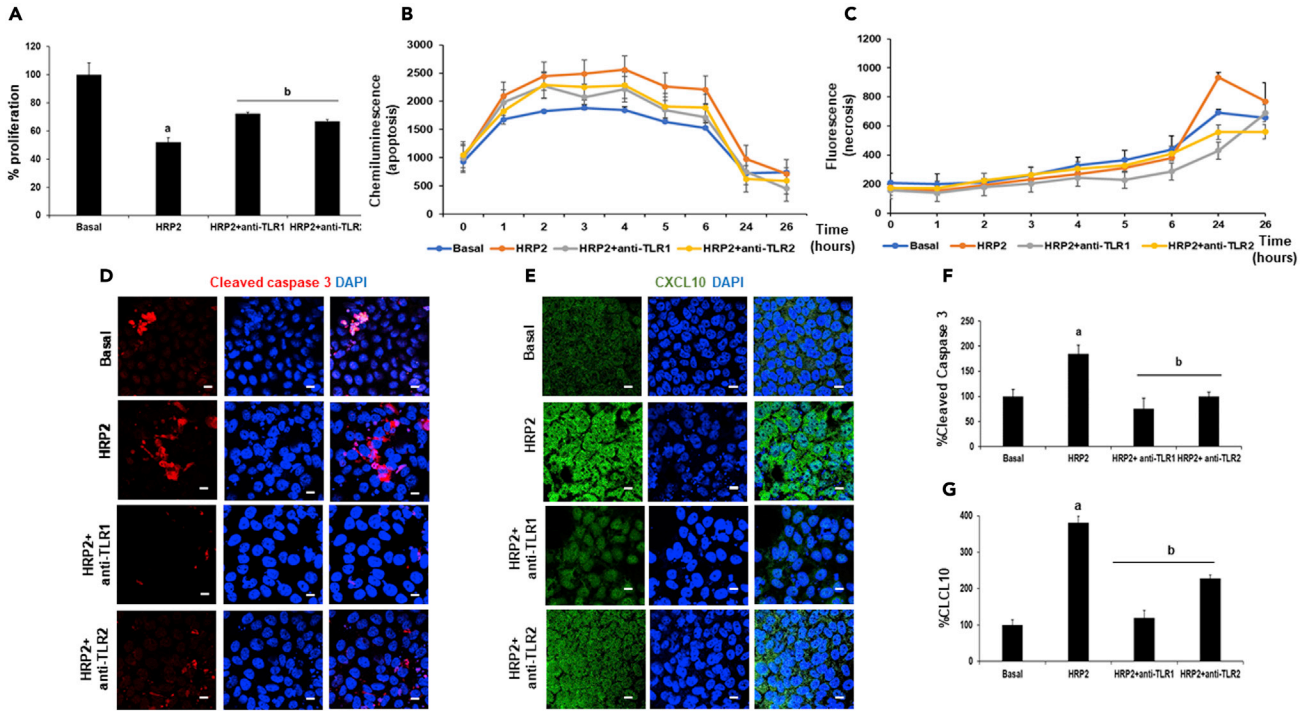

Figure 7. HRP2 uses TLR1 and TLR2 to increase CXCL10 expression and cell death in iPSC

Cell proliferation, apoptosis, and expression of inflammatory markers were assessed in iPSC treated with HRP2 after TLR1 and TLR2 blockage.
(A) Proliferation assay showed that IPSC growth was partially restored, whereas their apoptosis (B) and necrosis (C) were reduced to the levels of untreated controls. TLR1 and TLR2 blocking in HRP2-treated iPSC has an antiapoptotic and anti-inflammatory effect, as it is confirmed by IHC: the expression of cleaved caspase 3 (D, F) and CXCL10 (E, G) is reduced. Data represented as means ± SEM a: $p < 0.05$ compared to basal conditions; b: $p < 0.05$ compared to HRP2 treatment. Statistical significance between groups was determined using *t*-test and analysis of variance.

postmortem samples provided only cross-sectional information, it has been impossible to investigate the injury/repair processes during recovery after HCM treatment. Various studies have used brain organoids derived from iPSC that retain the genomic background, cellular organization, and functionality of their tissue-of-origin. In recent studies of Zika virus infection in organoids, it was found to cause neuronal cell death in early stages of brain development (Garcez et al., 2016) and premature differentiation of neuronal stem cells (Gabriel et al., 2017). Another study reported that SARS-CoV-2, the virus responsible for COVID-19, preferably targets neurons using brain organoids (Ramani et al., 2020), which was confirmed by the detection of the virus in cortical neurons from postmortem brain samples (Song et al., 2021). We have previously used $CD34^+$ cord blood-derived iPSC and cortical organoids featuring neurons, neuronal stem cells, astrocytes, and microglia to demonstrate that heme contributed significantly to brain damage (Harbuzariu et al., 2019).

Here, we report that HRP2, a parasite-derived factor, induced neuronal apoptosis (Figures 2–4) and inflammation (Figures 5–7) in an iPSC-derived brain organoids model. To functionally determine that HRP2 specifically affects iPSC proliferation, we used a neutralizing antibody (anti-HRP2), which abolished the loss-of-proliferation of iPSCs (Figure 1). Moreover, when iPSCs were treated with random proteins containing L-histidine, they did not impact cell proliferation, viability, or pluripotency and had a slight pro-inflammatory effect, although not significant. HRP2 disrupted the forebrain structures and activated the extrinsic apoptotic pathway by augmenting cleaved caspase 3 and 8, as well as PARP expression. NRG1 protected the cells against HRP2 apoptotic effects (Figures 2 and 3). In addition, the neuroprotective effects of NRG1 diminished when ErbB4 was blocked, suggesting that NRG1 specific effects in promoting iPSC growth and pluripotency may be modulated through this receptor. This study has revealed that HRP2 induces structural modifications, cellular apoptosis, and neuroinflammation in cortical organoids that is attenuated by NRG1.

Two of the main events that NF-kB regulates are apoptosis and inflammation. In mammals, the NF-kB family is composed of five transcription factors: p50, p52, p65 (RelA), c-Rel, and RelB. Unlike p65, p50 lacks the

transcription activation domain and needs to form heterodimers with p65, c-Rel, or RelB to target gene expression. Other groups have demonstrated that although activation of NF-κB and apoptosis occurred in neurons and glial cells in fatal HCM, there is no correlation between NF-κB p65 expression and cleaved caspase-3, suggesting that the NF-κB p65 signaling pathway may not be the main culprit for neuronal and glial cell apoptosis in HCM (Punsawad et al., 2013). Our results show that p50 expression was significantly increased by HRP2 and correlated with cleaved caspase-3 expression, suggesting that it could be involved in neuronal and astrocytic apoptosis (Figures 2 and 3) in brain organoids. Further investigations of NF-kB involvement in HRP2-induced apoptosis should be conducted using p50 knockouts and should also target p50/RelB or p50/c-Rel dimers.

Immediately following traumatic brain injury, rats display neuronal BDNF upregulation around damaged hippocampus and brain cortex areas (Griesbach et al., 2002; Hicks et al., 1999). As the severity of ECM increased, BDNF mRNA progressively decreased, while IHC showed changes in neuronal BDNF distribution pattern, suggesting altered axonal transport in the brain cortex of ECM mice (Linares et al., 2013). We have shown that short-term exposure to heme and HRP2 increased BDNF neuronal expression in cortical organoids, which might protect against their apoptosis-induced damage. NFL is unique to neuronal cells and is increased not only in CSF following brain damage in multiple sclerosis but also in the serum of elderly people (Khalil et al., 2020). NFM was increased in the CSF and serum of patients with brain damage (Martinez-Morillo et al., 2015). We have demonstrated that NFM expression — and not NFL — is decreased by HRP2 treatment (Figure 4). Future studies using choroid plexus organoids (Giandomenico et al., 2019) could be used to investigate whether NFM reduced brain cortical expression correlates with increased levels in CSF following HRP2-induced injury.

The CXCL10, Ang-2 and Ang-2: Ang-1 ratio are predictive biomarkers of HCM pathogenesis that can be used for predicting HCM severity (Jain et al., 2011; Wilson et al., 2011). Indeed, both heme and HRP2 similarly increase the expression of CXCL10 and Ang-2: Ang-1 ratio, whereas NRG1 decreases pro-inflammatory marker expression (Figure 5). We have confirmed HRP2 effects by showing that inflammation-related, apoptosis-related, and brain developmental-related gene expressions in 50-day-old brain cortical organoids (Figure 6) were modified. Among these genes, the TLR1 and 2-related signaling stood out, suggesting that there is a tight association between HRP2 and TLRs, which may function as HRP2 receptors. Indeed, our functional studies conducted in iPSC (Figure 7) demonstrate that when TLR1 and TLR2 are blocked by monoclonal antibodies, the HRP2-induced cellular damage is reduced. Interestingly, although the HRP2-induced iPSC apoptosis is abrogated by TLR1 and TLR2 blockage, the inflammatory effects are only partially diminished, suggesting that other pathways may be involved.

Limitations of the study

Brain organoids recapitulate some aspects of the *in vivo* fetal brain tissue, including its architecture and cellular composition. However, this model presents a few limitations, including immature neuronal function and variations between organoid batches in the number and size of the ventricle-like forebrain structures (Kim et al., 2021). Because human brain tissue is notoriously difficult to obtain, we used brain organoids as a model to investigate whether HRP2 induces cellular damage in microglia, neurons, and astrocytes. We are aware of the immaturity of these fetal-stage neuronal tissues and realize that it is possible that more mature, adult-stage neuronal cells are more resistant. However, previous studies using postmortem brain tissue from children that died from HCM have shown that neuronal cell damage occurs, but it is impossible to determine how much of this injury is because of HRP2 alone or to other pro-inflammatory factors (e.g., CXCL10, heme, etc.) that may cross the leaky BBB during late stages of the disease. Another limitation of this study is the lack of organoid vascularization. However, these studies were specifically aimed to understand what happens with brain cortical cells away from the vascular system. In the future, we will use patient-derived neurovascular units (organ on a chip) to understand the mechanisms of malaria-induced brain cellular injury in the perivascular space. The studies presented in this manuscript provide some answers to these questions; however, further investigations are necessary to fully understand HCM pathogenesis and to identify new therapeutic targets against brain tissue damage.

STAR★METHODS

Detailed methods are provided in the online version of this paper and include the following:

SUPPLEMENTAL INFORMATION

Supplemental information can be found online at https://doi.org/10.1016/j.isci.2022.104407.

ACKNOWLEDGMENTS

We wish to acknowledge the technical assistance, service, and expertise provided by the core facilities of the Parker H. Petit Institute for Bioengineering and Bioscience at Georgia Institute of Technology (Histology core; Ms. Sh'Aqua Asberry and Microscopy core; Mr. Andrew Shaw). This work was supported by the National Institutes of Health grants NIH/NINDS R01NS091616 and R01NS125775-01, NIH/RCMI (2U54) MD007602-31, NIH/FIC 1K01TW010282, NIH/FIC 5R25TW009340, NIH/NCATS TL1TR002382 and Georgia Clinical and Translational Science Alliance (GCTSA).

AUTHOR CONTRIBUTIONS

J.K.S. and A.H. designed the research. A.H., A.N., and J.C.C. performed the research. A.H., A.N., K.O.H., J.C.C., and A.D. analyzed the data. J.K.S. and A.H. wrote the paper.

DECLARATION OF INTERESTS

The authors declare no competing interests.

INCLUSION AND DIVERSITY

One or more of the authors of this paper self-identifies as an underrepresented ethnic minority in science. While citing references scientifically relevant for this work, we also actively worked to promote gender balance in our reference list.

Received: May 30, 2021
Revised: December 21, 2021
Accepted: May 11, 2022
Published: June 17, 2022

REFERENCES

Armah, H., Dodoo, A.K., Wiredu, E.K., Stiles, J.K., Adjei, A.A., Gyasi, R.K., and Tettey, Y. (2005). High-level cerebellar expression of cytokines and adhesion molecules in fatal, paediatric, cerebral malaria. Ann. Trop. Med. Parasitol. *99*, 629–647. https://doi.org/10.1179/136485905x51508.

Armah, H.B., Wilson, N.O., Sarfo, B.Y., Powell, M.D., Bond, V.C., Anderson, W., Adjei, A.A., Gyasi, R.K., Tettey, Y., Wiredu, E.K., et al. (2007). Cerebrospinal fluid and serum biomarkers of cerebral malaria mortality in Ghanaian children. Malar. J. *6*, 147. https://doi.org/10.1186/1475-2875-6-147.

Bangirana, P., Opoka, R.O., Boivin, M.J., Idro, R., Hodges, J.S., and John, C.C. (2016). Neurocognitive domains affected by cerebral malaria and severe malarial anemia in children. Learn. Individ. Differ. *46*, 38–44. https://doi.org/10.1016/j.lindif.2015.01.010.

Burridge, P.W., Thompson, S., Millrod, M.A., Weinberg, S., Yuan, X., Peters, A., Mahairaki, V., Koliatsos, V.E., Tung, L., and Zambidis, E.T. (2011). A universal system for highly efficient cardiac differentiation of human induced pluripotent stem cells that eliminates interline

variability. PLoS. One. *6*, e18293. https://doi.org/10.1371/journal.pone.0018293.

Bylicka-Szczepanowska, E., and Korzeniewski, K. (2022). Asymptomatic malaria infections in the time of COVID-19 pandemic: experience from the central african republic. Int. J. Environ. Res. Publ. Health *19*, 3544. https://doi.org/10.3390/ijerph19063544.

Cacialli, P., Palladino, A., and Lucini, C. (2018). Role of brain-derived neurotrophic factor during the regenerative response after traumatic brain injury in adult zebrafish. Neural Regen Res *13*, 941–944. https://doi.org/10.4103/1673-5374.233430.

Campos, M.A.S., Almeida, I.C., Takeuchi, O., Akira, S., Valente, E.P., Procopio, D.O., Travassos, L.R., Smith, J.A., Golenbock, D.T., and Gazzinelli, R.T. (2001). Activation of Toll-like receptor-2 by glycosylphosphatidylinositol anchors from a protozoan parasite. J. Immunol. *167*, 416–423. https://doi.org/10.4049/jimmunol.167.1.416.

Chen, Y.J., Zhang, M., Yin, D.M., Wen, L., Ting, A., Wang, P., Lu, Y.S., Zhu, X.H., Li, S.J., Wu, C.Y., et al. (2010). ErbB4 in parvalbumin-positive interneurons is critical for neuregulin 1 regulation of long-term potentiation. Proc. Natl. Acad. Sci. U S A. *107*, 21818–21823. https://doi.org/10.1073/pnas.1010669107.

Cruz-Orengo, L., Daniels, B.P., Dorsey, D., Basak, S.A., Grajales-Reyes, J.G., McCandless, E.E., Piccio, L., Schmidt, R.E., Cross, A.H., Crosby, S.D., and Klein, R.S. (2014). Enhanced sphingosine-1-phosphate receptor 2 expression underlies female CNS autoimmunity susceptibility. J. Clin. Invest. *124*, 2571–2584. https://doi.org/10.1172/jci73408.

Dalrymple, U., Arambepola, R., Gething, P.W., and Cameron, E. (2018). How long do rapid diagnostic tests remain positive after anti-malarial treatment? Malar. J. *17*, 228. https://doi.org/10.1186/s12936-018-2371-9.

Daniels, B.P., Cruz-Orengo, L., Pasieka, T.J., Couraud, P.O., Romero, I.A., Weksler, B., Cooper, J.A., Doering, T.L., and Klein, R.S. (2013). Immortalized human cerebral microvascular endothelial cells maintain the properties of primary cells in an in vitro model of immune migration across the blood brain barrier. J. Neurosci. Methods. *212*, 173–179. https://doi.org/10.1016/j.jneumeth.2012.10.001.

Das, P., Grewal, J.S., and Chauhan, V.S. (2006). Interaction of Plasmodium falciparum histidine-rich protein II with human lymphocytes leads to suppression of proliferation, IFN-gamma release, and CD69 expression. Parasitol. Res. *100*, 39–50. https://doi.org/10.1007/s00436-006-0228-6.

Brian de Souza, J., and Riley, E.M. (2002). Cerebral malaria: the contribution of studies in animal models to our understanding of immunopathogenesis. Microbes Infect. *4*, 291–300. https://doi.org/10.1016/s1286-4579(02)01541-1.

Doolan, D.L., Dobaño, C., and Baird, J.K. (2009). Acquired immunity to malaria. Clin. Microbiol. Rev. *22*, 13–36. https://doi.org/10.1128/cmr.00025-08.

Dorovini-Zis, K., Schmidt, K., Huynh, H., Fu, W., Whitten, R.O., Milner, D., Kamiza, S., Molyneux, M., and Taylor, T.E. (2011). The neuropathology of fatal cerebral malaria in malawian children. Am. J. Pathol. *178*, 2146–2158. https://doi.org/10.1016/j.ajpath.2011.01.016.

Dutra, F.F., Alves, L.S., Rodrigues, D., Fernandez, P.L., de Oliveira, R.B., Golenbock, D.T., Zamboni, D.S., and Bozza, M.T. (2014). Hemolysis-induced lethality involves inflammasome activation by heme. Proc. Natl. Acad. Sci. U S A. *111*, E4110–E4118. https://doi.org/10.1073/pnas.1405023111.

Fernando, D., de Silva, D., Carter, R., Mendis, K.N., and Wickremasinghe, R. (2006). A randomized, double-blind, placebo-controlled, clinical trial of the impact of malaria prevention on the educational attainment of school children. Am. J. Trop. Med. Hyg. *74*, 386–393. https://doi.org/10.4269/ajtmh.2006.74.386.

Flames, N., Long, J.E., Garratt, A.N., Fischer, T.M., Gassmann, M., Birchmeier, C., Lai, C., Rubenstein, J.L., and Marin, O. (2004). Short- and long-range attraction of cortical GABAergic interneurons by neuregulin-1. Neuron *44*, 251–261. https://doi.org/10.1016/j.neuron.2004.09.028.

Fox, L.L., Taylor, T.E., Pensulo, P., Liomba, A., Mpakiza, A., Varela, A., Glover, S.J., Reeves, M.J., and Seydel, K.B. (2013). Histidine-rich protein 2 plasma levels predict progression to cerebral malaria in Malawian children with Plasmodium falciparum infection. J. Infect. Dis. *208*, 500–503. https://doi.org/10.1093/infdis/jit176.

Gabriel, E., Ramani, A., Karow, U., Gottardo, M., Natarajan, K., Gooi, L.M., Goranci-Buzhala, G., Krut, O., Peters, F., Nikolic, M., et al. (2017). Recent Zika virus isolates induce premature differentiation of neural progenitors in human brain organoids. Cell. Stem. Cell. *20*, 397–406.e5. https://doi.org/10.1016/j.stem.2016.12.005.

Garcez, P.P., Loiola, E.C., Madeiro da Costa, R., Higa, L.M., Trindade, P., Delvecchio, R., Nascimento, J.M., Brindeiro, R., Tanuri, A., and Rehen, S.K. (2016). Zika virus impairs growth in human neurospheres and brain organoids. Science *352*, 816–818. https://doi.org/10.1126/science.aaf6116.

Giandomenico, S.L., Mierau, S.B., Gibbons, G.M., Wenger, L.M.D., Masullo, L., Sit, T., Sutcliffe, M., Boulanger, J., Tripodi, M., Derivery, E., et al. (2019). Cerebral organoids at the air-liquid interface generate diverse nerve tracts with functional output. Nat. Neurosci. *22*, 669–679. https://doi.org/10.1038/s41593-019-0350-2.

Griesbach, G.S., Hovda, D.A., Molteni, R., and Gomez-Pinilla, F. (2002). Alterations in BDNF and synapsin I within the occipital cortex and hippocampus after mild traumatic brain injury in the developing rat: reflections of injury-induced neuroplasticity. J. Neurotrauma *19*, 803–814. https://doi.org/10.1089/08977150260190401.

Harbuzariu, A., Pitts, S., Cespedes, J.C., Harp, K.O., Nti, A., Shaw, A.P., Liu, M., and Stiles, J.K. (2019). Modelling heme-mediated brain injury associated with cerebral malaria in human brain cortical organoids. Sci. Rep. *9*, 19162. https://doi.org/10.1038/s41598-019-55631-8.

Hendriksen, I.C.E., Mwanga-Amumpaire, J., von Seidlein, L., Mtove, G., White, L.J., Olaosebikan, R., Lee, S.J., Tshefu, A.K., Woodrow, C., Amos, B., et al. (2012). Diagnosing severe falciparum malaria in parasitaemic African children: a prospective evaluation of plasma PfHRP2 measurement. PLoS Med. *9*, e1001297. https://doi.org/10.1371/journal.pmed.1001297.

Hicks, R.R., Martin, V.B., Zhang, L., and Seroogy, K.B. (1999). Mild experimental brain injury differentially alters the expression of neurotrophin and neurotrophin receptor mRNAs in the hippocampus. Exp. Neurol. *160*, 469–478. https://doi.org/10.1006/exnr.1999.7216.

Hunt, N.H., Golenser, J., Chan-Ling, T., Parekh, S., Rae, C., Potter, S., Medana, I.M., Miu, J., and Ball, H.J. (2006). Immunopathogenesis of cerebral malaria. Int. J. Parasitol. *36*, 569–582. https://doi.org/10.1016/j.ijpara.2006.02.016.

Idro, R., Kakooza-Mwesige, A., Balyejjussa, S., Mirembe, G., Mugasha, C., Tugumisirize, J., and Byarugaba, J. (2010). Severe neurological sequelae and behaviour problems after cerebral malaria in Ugandan children. BMC Res. Notes. *3*, 104. https://doi.org/10.1186/1756-0500-3-104.

Imwong, M., Woodrow, C.J., Hendriksen, I.C.E., Veenemans, J., Verhoef, H., Faiz, M.A., Mohanty, S., Mishra, S., Mtove, G., Gesase, S., et al. (2015). Plasma concentration of parasite DNA as a measure of disease severity in falciparum malaria. J. Infect. Dis. *211*, 1128–1133. https://doi.org/10.1093/infdis/jiu590.

Jain, V., Lucchi, N.W., Wilson, N.O., Blackstock, A.J., Nagpal, A.C., Joel, P.K., Singh, M.P., Udhayakumar, V., Stiles, J.K., and Singh, N. (2011). Plasma levels of angiopoietin-1 and -2 predict cerebral malaria outcome in Central India. Malar. J. *10*, 383. https://doi.org/10.1186/1475-2875-10-383.

Kariuki, S.M., Gitau, E., Gwer, S., Karanja, H.K., Chengo, E., Kazungu, M., Urban, B.C., and Newton, C.R.J.C. (2014). Value of Plasmodium falciparum histidine-rich protein 2 level and malaria retinopathy in distinguishing cerebral malaria from other acute encephalopathies in Kenyan children. J. Infect. Dis. *209*, 600–609. https://doi.org/10.1093/infdis/jit500.

Khalil, M., Pirpamer, L., Hofer, E., Voortman, M.M., Barro, C., Leppert, D., Benkert, P., Ropele, S., Enzinger, C., Fazekas, F., et al. (2020). Serum neurofilament light levels in normal aging and their association with morphologic brain changes. Nat. Commun. *11*, 812. https://doi.org/10.1038/s41467-020-14612-6.

Kim, J., Sullivan, G.J., and Park, I.H. (2021). How well do brain organoids capture your brain? iScience *24*, 102063. https://doi.org/10.1016/j.isci.2021.102063.

Lancaster, M.A., Corsini, N.S., Wolfinger, S., Gustafson, E.H., Phillips, A.W., Burkard, T.R., Otani, T., Livesey, F.J., and Knoblich, J.A. (2017). Guided self-organization and cortical plate formation in human brain organoids. Nat. Biotechnol. *35*, 659–666. https://doi.org/10.1038/nbt.3906.

Lancaster, M.A., Renner, M., Martin, C.A., Wenzel, D., Bicknell, L.S., Hurles, M.E., Homfray, T., Penninger, J.M., Jackson, A.P., and Knoblich, J.A. (2013). Cerebral organoids model human brain development and microcephaly. Nature *501*, 373–379. https://doi.org/10.1038/nature12517.

Linares, M., Marin-Garcia, P., Perez-Benavente, S., Sanchez-Nogueiro, J., Puyet, A., Bautista, J.M., and Diez, A. (2013). Brain-derived neurotrophic factor and the course of experimental cerebral malaria. Brain Res. *1490*, 210–224. https://doi.org/10.1016/j.brainres.2012.10.040.

Liu, M., Solomon, W., Cespedes, J.C., Wilson, N.O., Ford, B., and Stiles, J.K. (2018). Neuregulin-1 attenuates experimental cerebral malaria (ECM) pathogenesis by regulating ErbB4/AKT/STAT3 signaling. J. Neuroinflammation. *15*, 104. https://doi.org/10.1186/s12974-018-1147-z.

Lopez-Bendito, G., Cautinat, A., Sanchez, J.A., Bielle, F., Flames, N., Garratt, A.N., Talmage, D.A., Role, L.W., Charnay, P., Marin, O., and Garel, S. (2006). Tangential neuronal migration controls axon guidance: a role for neuregulin-1 in thalamocortical axon navigation. Cell *125*, 127–142. https://doi.org/10.1016/j.cell.2006.01.042.

Lovegrove, F.E., Tangpukdee, N., Opoka, R.O., Lafferty, E.I., Rajwans, N., Hawkes, M., Krudsood, S., Looareesuwan, S., John, C.C., Liles, W.C., and Kain, K.C. (2009). Serum angiopoietin-1 and -2 levels discriminate cerebral malaria from uncomplicated malaria and predict clinical outcome in African children. PLoS. One. *4*, e4912. https://doi.org/10.1371/journal.pone.0004912.

Mages, B., Aleithe, S., Altmann, S., Blietz, A., Nitzsche, B., Barthel, H., Horn, A.K.E., Hobusch, C., Hartig, W., Krueger, M., and Michalski, D. (2018). Impaired neurofilament integrity and neuronal morphology in different models of focal cerebral ischemia and human stroke tissue. Front. Cell. Neurosci. *12*, 161. https://doi.org/10.3389/fncel.2018.00161.

Martinez-Morillo, E., Childs, C., Garcia, B.P., Alvarez Menendez, F.V., Romaschin, A.D., Cervellin, G., Lippi, G., and Diamandis, E.P. (2015). Neurofilament medium polypeptide (NFM) protein concentration is increased in CSF and serum samples from patients with brain injury. Clin. Chem. Lab. Med. *53*, 1575–1584. https://doi.org/10.1515/cclm-2014-0908.

McDonald, C.R., Conroy, A.L., Hawkes, M., Elphinstone, R.E., Gamble, J.L., Hayford, K., Namasopo, S., Opoka, R.O., Liles, W.C., and Kain, K.C. (2017). Brain-derived neurotrophic factor is associated with disease severity and clinical outcome in Ugandan children admitted to hospital with severe malaria. Pediatr. Infect. Dis. J. *36*, 146–150. https://doi.org/10.1097/inf.0000000000001382.

Medana, I.M., Day, N.P., Hien, T.T., Mai, N.T.H., Bethell, D., Phu, N.H., Farrar, J., Esiri, M.M., White, N.J., and Turner, G.D. (2002). Axonal injury in cerebral malaria. Am. J. Pathol. *160*, 655–666. https://doi.org/10.1016/s0002-9440(10)64885-7.

Mikita, K., Thakur, K., Anstey, N.M., Piera, K.A., Pardo, C.A., Weinberg, J.B., Mukemba, J., Sullivan, D.J., Mwaikambo, E.D., Granger, D.L., et al. (2014). Quantification of Plasmodium falciparum histidine-rich protein-2 in cerebrospinal spinal fluid from cerebral malaria patients. Am. J. Trop. Med. Hyg. *91*, 486–492. https://doi.org/10.4269/ajtmh.14-0210.

Milner, D.A., Jr., Whitten, R.O., Kamiza, S., Carr, R., Liomba, G., Dzamalala, C., Seydel, K.B., Molyneux, M.E., and Taylor, T.E. (2014). The systemic pathology of cerebral malaria in African children. Front. Cell. Infect. Microbiol. *4*, 104. https://doi.org/10.3389/fcimb.2014.00104.

Ormel, P.R., Vieira de Sa, R., van Bodegraven, E.J., Karst, H., Harschnitz, O., Sneeboer, M.A.M., Johansen, L.E., van Dijk, R.E., Scheefhals, N., Berdenis van Berlekom, A., et al. (2018). Microglia innately develop within cerebral organoids. Nat. Commun. *9*, 4167. https://doi.org/10.1038/s41467-018-06684-2.

Pal, P., Balaban, A.E., Diamond, M.S., Sinnis, P., Klein, R.S., and Goldberg, D.E. (2017). Plasmodium falciparum histidine-rich protein II causes vascular leakage and exacerbates experimental cerebral malaria in mice. PLoS One. *12*, e0177142. https://doi.org/10.1371/journal.pone.0177142.

Pal, P., Daniels, B.P., Oskman, A., Diamond, M.S., Klein, R.S., and Goldberg, D.E. (2016). Plasmodium falciparum histidine-rich protein II compromises brain endothelial barriers and may promote cerebral malaria pathogenesis. mBio *7*. https://doi.org/10.1128/mbio.00617-16.

Petryshen, T.L., Middleton, F.A., Kirby, A., Aldinger, K.A., Purcell, S., Tahl, A.R., Morley, C.P., McGann, L., Gentile, K.L., Rockwell, G.N., et al. (2005). Support for involvement of neuregulin 1 in schizophrenia pathophysiology. Mol Psychiatry *10*, 366–374. https://doi.org/10.1038/sj.mp.4001608.

Phillips, R.E., and Solomon, T. (1990). Cerebral malaria in children. Lancet *336*, 1355–1360. https://doi.org/10.1016/0140-6736(90)92903-u.

Poti, K.E., Sullivan, D.J., Dondorp, A.M., and Woodrow, C.J. (2020). HRP2: transforming malaria diagnosis, but with caveats. Trends Parasitol. *36*, 112–126. https://doi.org/10.1016/j.pt.2019.12.004.

Prapansilp, P., Medana, I., Mai, N.T.H., Day, N.P., Phu, N.H., Yeo, T.W., Hien, T.T., White, N.J., Anstey, N.M., and Turner, G.D. (2013). A clinicopathological correlation of the expression of the angiopoietin-Tie-2 receptor pathway in the brain of adults with Plasmodium falciparum malaria. Malar. J. *12*, 50. https://doi.org/10.1186/1475-2875-12-50.

Punsawad, C., Maneerat, Y., Chaisri, U., Nantavisai, K., and Viriyavejakul, P. (2013). Nuclear factor kappa B modulates apoptosis in the brain endothelial cells and intravascular leukocytes of fatal cerebral malaria. Malar. J. *12*, 260. https://doi.org/10.1186/1475-2875-12-260.

Quintanilla, R.H., Jr., Asprer, J.S.T., Vaz, C., Tanavde, V., and Lakshmipathy, U. (2014). CD44 is a negative cell surface marker for pluripotent stem cell identification during human fibroblast reprogramming. PLoS One. *9*, e85419. https://doi.org/10.1371/journal.pone.0085419.

Ramani, A., Muller, L., Ostermann, P.N., Gabriel, E., Abida-Islam, P., Muller-Schiffmann, A., Mariappan, A., Goureau, O., Gruell, H., Walker, A., et al. (2020). SARS-CoV-2 targets neurons of 3D human brain organoids. EMBO J. *39*, e106230. https://doi.org/10.15252/embj.2020106230.

Renia, L., Howland, S.W., Claser, C., Gruner, A.C., Suwanarusk, R., Teo, T.H., Russell, B., and Ng, L.F. (2012). Cerebral malaria: mysteries at the blood-brain barrier. Virulence *3*, 193–201. https://doi.org/10.4161/viru.19013.

Renner, M., Lancaster, M.A., Bian, S., Choi, H., Ku, T., Peer, A., Chung, K., and Knoblich, J.A. (2017). Self-organized developmental patterning and differentiation in cerebral organoids. EMBO J. *36*, 1316–1329. https://doi.org/10.15252/embj.201694700.

Reuterswärd, P., Bergström, S., Orikiiriza, J., Lindquist, E., Bergström, S., Andersson Svahn, H., Ayoglu, B., Uhlén, M., Wahlgren, M., Normark, J., Ribacke, U., and Nilsson, P. (2018). Levels of human proteins in plasma associated with acute paediatric malaria. Malaria journal *17*, 426. 30442134. https://doi.org/10.1186/s12936-018-2576-y.

Rubach, M.P., Mukemba, J., Florence, S., John, B., Crookston, B., Lopansri, B.K., Yeo, T.W., Piera, K.A., Alder, S.C., Weinberg, J.B., et al. (2012). Plasma Plasmodium falciparum histidine-rich protein-2 concentrations are associated with malaria severity and mortality in Tanzanian children. PLoS. One. *7*, e35985. https://doi.org/10.1371/journal.pone.0035985.

Simmons, L.J., Surles-Zeigler, M.C., Li, Y., Ford, G.D., Newman, G.D., and Ford, B.D. (2016). Regulation of inflammatory responses by neuregulin-1 in brain ischemia and microglial cells in vitro involves the NF-kappa B pathway. J. Neuroinflammation *13*, 237. https://doi.org/10.1186/s12974-016-0703-7.

Soares, M.P., and Weiss, G. (2015). The Iron age of host-microbe interactions. EMBO. Rep. *16*, 1482–1500. https://doi.org/10.15252/embr.201540558.

Solomon, W., Wilson, N.O., Anderson, L., Pitts, S., Patrickson, J., Liu, M., Ford, B.D., and Stiles, J.K. (2014). Neuregulin-1 attenuates mortality associated with experimental cerebral malaria. J. Neuroinflammation. *11*, 9. https://doi.org/10.1186/1742-2094-11-9.

Song, E., Zhang, C., Israelow, B., Lu-Culligan, A., Prado, A.V., Skriabine, S., Lu, P., Weizman, O.E., Liu, F., Dai, Y., et al. (2021). Neuroinvasion of SARS-CoV-2 in human and mouse brain. J. Exp. Med. *218*, e20202135. https://doi.org/10.1084/jem.20202135.

Storm, J., Jespersen, J.S., Seydel, K.B., Szestak, T., Mbewe, M., Chisala, N.V., Phula, P., Wang, C.W., Taylor, T.E., Moxon, C.A., et al. (2019). Cerebral malaria is associated with differential cytoadherence to brain endothelial cells. EMBO Mol. Med. *11*, e9164. https://doi.org/10.15252/emmm.201809164.

Tripathi, A.K., Sullivan, D.J., and Stins, M.F. (2007). Plasmodium falciparum-infected erythrocytes decrease the integrity of human blood-brain barrier endothelial cell monolayers. J. Infect. Dis. *195*, 942–950. https://doi.org/10.1086/512083.

Wilson, N.O., Huang, M.B., Anderson, W., Bond, V., Powell, M., Thompson, W.E., Armah, H.B.,

Adjei, A.A., Gyasi, R., Tettey, Y., et al. (2008). Soluble factors from Plasmodium falciparum-infected erythrocytes induce apoptosis in human brain vascular endothelial and neuroglia cells. Mol. Biochem. Parasitol. *162*, 172–176. https://doi.org/10.1016/j.molbiopara.2008.09.003.

Wilson, N.O., Jain, V., Roberts, C.E., Lucchi, N., Joel, P.K., Singh, M.P., Nagpal, A.C., Dash, A.P., Udhayakumar, V., Singh, N., and Stiles, J.K. (2011). CXCL4 and CXCL10 predict risk of fatal cerebral malaria. Dis. Markers. *30*, 39–49. https://doi.org/10.1155/2011/828256.

Yau, H.J., Wang, H.F., Lai, C., and Liu, F.C. (2003). Neural development of the neuregulin receptor ErbB4 in the cerebral cortex and the hippocampus: preferential expression by interneurons tangentially migrating from the ganglionic eminences. Cereb Cortex. *13*, 252–264. https://doi.org/10.1093/cercor/13.3.252.

Zhao, X., and Bhattacharyya, A. (2018). Human models are needed for studying human neurodevelopmental disorders. Am. J. Hum. Genet. *103*, 829–857. https://doi.org/10.1016/j.ajhg.2018.10.009.

STAR★METHODS

KEY RESOURCES TABLE

REAGENT or RESOURCE	SOURCE	IDENTIFIER
Antibodies		
Mouse monoclonal anti-human Ki 67, clone B56	BD Biosciences	Cat # 550,609, RRID: AB_393778
Goat polyclonal anti-human Sox-2	R&D Systems	Cat #AF2018 RRID: AB_355110
Sheep anti-Rabbit IgG (whole molecule), F(ab')2 fragment–Cy3 secondary antibody	Sigma	Cat #C2306 RRID: AB_258792
Goat anti-Mouse IgG, IgM (H + L) Secondary Antibody, Alexa Fluor 488	Thermo Fisher Scientific	Cat # A-10680 RRID: AB_2534062
Mouse monoclonal anti-human Tubulin β 3 (TUBB3) Antibody, Clone TUJ1	BioLegend; (previously Covance# MMS-435P)	Cat #801201 RRID: AB_2313773
Rabbit polyclonal anti-human IBA1 antibody	Fujifilm Wako Chemicals USA Corp	Cat # 019-19,741 RRID: AB_839504
Rabbit polyclonal anti-human NRG1 antibody	Abcam	Cat # ab180808 RRID: AB_2732881
Rabbit monoclonal anti-human ErbB4/HER4	Abcam	Cat # ab32375 RRID: AB_731579
Rabbit polyclonal anti-human GFAP	Abcam	Cat # ab7260 RRID: AB_305808
Mouse monoclonal anti-human Angiopoietin 2 antibody, clone #MM0020-1F29	Abcam	Cat # ab56301 RRID: AB_2226229
Rabbit polyclonal to human Angiopoietin 1 antibody	Abcam	Cat # ab94684 RRID: AB_10677472
Goat polyclonal anti-human Brachyury antibody	R&D Systems	Cat #AF-2085 RRID: AB_2200235
Donkey anti-goat Alexa Fluor 488 secondary antibody	Fisher Scientific	Cat # PIA32814TR RRID: AB_2866497
Rabbit monoclonal anti-human cleaved caspase 3, clone D3E9	Cell Signaling	Cat #9579S RRID: AB_10897512
Rabbit monoclonal anti-human Neurofilament-L (clone C28E10)	Cell Signaling	Cat # 2837S RRID: AB_823575
Mouse monoclonal anti-human Neurofilament-M (clone RMO 14.9)	Cell Signaling	Cat #2838S RRID: AB_561191
Rabbit polyclonal anti-human BDNF	Thermo Fisher Scientific	Cat #PA5-85730 RRID: AB_2792869
Rabbit polyclonal anti-human CXCL10	PeproTech	Cat #500-P93 RRID: AB_148035
Rabbit anti-Human CXCR3 Polyclonal	Abcam	Cat #ab133420 RRID: AB_11154962
Mouse monoclonal anti-protozoa HRP2	Fisher Scientific	Cat #MA127094 RRID: AB_795202
Mouse monoclonal anti-human NF-kB (clone E-10)	Santa Cruz Biotechnology	Cat # 8414 RRID: AB_628015
Mouse monoclonal anti-human TLR4 (clone 25)	Santa Cruz Biotechnology	Cat # sc-293072 RRID: AB_10611320

(*Continued on next page*)

Continued

REAGENT or RESOURCE	SOURCE	IDENTIFIER
Mouse monoclonal anti-human Caspase 3 (clone 84803)	R&D Systems	Cat #MAB707 RRID: AB_2275223
Mouse monoclonal anti-human Caspase 8 (clone 84131)	R&D Systems	Cat # MAB704 RRID: AB_2068470
Rabbit monoclonal anti-human PARP (clone 46D11)	Cell Signaling	Cat #9532S RRID: AB_659884
Rabbit anti-human TLR1	Cell Signaling	Cat #2209T RRID: AB_2303485
Mouse anti-human TLR1 functional grade (clone GD2.F4)	Invitrogen	Cat #16-9911-82 RRID: AB_469275
Rabbit monoclonal anti-human TLR2 (clone D769Z)	Cell Signaling	Cat #12276T RRID: AB_2797867
Mouse anti-human TLR2 functional grade (clone TLR2.1)	Invitrogen	Cat # 16-9922-82 RRID: AB_469283
Rabbit monoclonal anti-human TLR3 (clone D10F10)	Cell Signaling	Cat #6961T RRID: AB_10829166
Rabbit polyclonal anti-human TLR5	Abcam	Cat #ab37071 RRID: AB_778504
Rabbit monoclonal anti-human TLR6 (clone D1Z88)	Cell Signaling	Cat #12717T RRID: AB_2798005
Rabbit monoclonal anti-human TLR7 (clone D7)	Cell Signaling	Cat #5632T RRID: AB_10692895
Rabbit monoclonal anti-human TLR8 (clone D326J)	Cell Signaling	Cat #11886T RRID: AB_2797755
Rabbit monoclonal anti-human TLR9 (clone D9M9H)	Cell Signaling	Cat #13674T RRID: AB_2798290
Rabbit monoclonal anti-human GAPDH-HRP	Cell Signaling	Cat #8884S RRID: AB_11129865
Rabbit monoclonal anti-human B-actin (clone	Cell Signaling	Cat #8457S RRID: AB_10950489
Goat polyclonal Anti-mouse HRP secondary	BioLegend	Cat #405306 RRID: AB_315009
Goat Anti-rabbit HRP conjugate secondary	Bio-Rad	Cat #170-6515 RRID: AB_2617112
Chemicals, peptides, and recombinant proteins		
Plasmodium falciparum HRP2	Bio-Rad	Cat #PIP001
Human NRG1-beta 1/HRG1-beta 1 EGF Domain Protein, Carrier Free	R&D Systems	Cat #396-HB-050/CF
L-histidine	Sigma	H6034
Poly L-histidine	Sigma	P9386
Y-27632	Stem Cell Technologies	Cat #72304, CAS# 129830-38-2
Triton X-100	Sigma	Cat # T8787
DPBS without Ca, Mg	Stem Cell Technologies	Cat # 37350
Paraformaldehyde Solution, 4% in PBS	Fisher Scientific	Cat # J19943, CAS#30525-89-4
10% BSA	Fisher Scientific	Cat # PI37525
Accutase solution	Stem Cell Technologies	Cat #07920
Corning Matrigel matrix for organoid culture, Phenol Red free, LDEV-free	Corning	Cat #356255

(*Continued on next page*)

Continued

REAGENT or RESOURCE	SOURCE	IDENTIFIER
Geltrex	Fisher Scientific	Cat #A1413301
STEMdiff Cerebral Organoid Kit	Stem Cell Technologies	Cat #08570
STEMdiff Cerebral Organoid Maturation Kit	Stem Cell Technologies	Cat #08571
Gibco Versene solution	Fisher Scientific	Cat # 15-040-066
Gibco Essential 8 Flex Medium Kit	Fisher Scientific	Cat # A2858501
Normal goat serum	Vector Laboratories	Cat # S-1000
Prolong gold anti-fade reagent with DAPI	Fisher Scientific	Cat # NC0581700
Vectashield mounting medium with DAPI	Vector Labs	Cat #H-1200-10
Critical commercial assays		
Cell counting kit-8 for cell proliferation/toxicity	Dojindo Molecular Technologies, Inc	Cat # CK04
RealTime-Glo Annexin V Apoptosis and Necrosis Assay	Promega	Cat #JA1011
Pierce BCA Protein Assay Kit	Fisher Scientific	Cat #PI23225
PARIS kit for RNA isolation	Fisher Scientific	Cat # AM1921
nCounter standard master kit	NanoString	Cat #NAA-AKIT-012
Deposited data		
Gene expression	This manuscript	NCBI GEO: GSE190750, token yfchycusfluvzct
Western blot	This manuscript	Mendeley data: https://doi.org/10.17632/74prtwkhkc.1
Experimental models: Cell lines		
Human Episomal Induced Pluripotent Stem Cells	Thermo Fisher Scientific	Cat #A18945
Brain cortical organoids	Jonathan K Stiles laboratory	https://doi.org/10.1038/s41598-019-55631-8; PMID: 31844087; PMCID: PMC6914785.
Software and algorithms		
Image J	NIH	https://imagej.nih.gov/ij/download.html RRID: SCR_003070
ZEN	Carl Zeiss Microscopy, LLC	https://www.zeiss.com/microscopy/us/products/microscope-software/zen.html RRID: SCR_018163
Microsoft Excel	Microsoft Office	RRID: SCR_016137
Other		
96-wells low attachment plates	Fisher Scientific	Cat # 07-201-680
24-wells low attachment plates	Fisher Scientific	Cat # 07-200-602
6-wells low attachment plates	Fisher Scientific	Cat # 07-200-601
60 mm low attachment dishes	Fisher Scientific	Cat # 05-539-100
Organoid embedding sheet	Stem cell technologies	Cat # 08579
Lab Tek 8 wells chamber slides	Fisher Scientific	Cat # 12-565-8
MycoProbe mycoplasma detection kit	R&D Systems	Cat#CUL001B

RESOURCE AVAILABILITY

Lead contact

Further information and requests for sources and reagents should be directed to the lead contact, Adriana Harbuzariu (adriana.harbuzariu@emory.edu).

Materials availability

All data are available in the manuscript text and supplemental information. iPSC line #A18945 is available from Thermo Fisher Scientific. Heme, HRP2 and NRG1 are commercially available. This study did not generate new unique reagents.

Data and code availability

- The gene arrays data generated during this study have been deposited and are publicly available at NCBI GEO: GSE190750 token yfchycusfluvzct. Accession numbers are also available in the Key resources table. Original Western blot images have been deposited at Mendeley Datasets(https://data.mendeley.com/datasets/74prtwkhkc/draft?a=812d2ab2-40bc-496d-b40a-7e4c39254250) and are publicly available as of the date of publication. The DOI is listed in the key resources table. Microscopy data reported in this paper will be shared by the lead contact upon request.
- The paper does not report original code
- All additional information required to reanalyze the data reported in this paper is available from the lead contact upon request

EXPERIMENTAL MODEL AND SUBJECT DETAILS

Plasmodium falciparum recombinant HRP2 (BioRad cat #PIP001, Hercules, CA) was prepared by expression in E.coli. The vehicle used for this protein is sodium carbonate buffer (ph = 9.6) with <0.1% sodium azide, while NRG1/carrier free (no bovine serum albumin added in its preparation) (Biotechne cat#377-HB-050/CF, Minneapolis, MN) is commercially available as lyophilized powder and was reconstituted in sterile PBS. As negative controls for HRP2, cells/organoids in basal condition were treated with the same dilution (~1:250) of HRP2 vehicle or 4.2 μg/ml L-histidine, and Poly L-histidine (Sigma, Burlington, MA). In addition, cells or organoids were treated with 4.2 μg/ml HRP2 (Storm et al., 2019) for 8 hours, then 100 ng/ml NRG1 (concentration within physiological range) was added (Liu et al., 2018) for 18 hours.

Induced pluripotent stem cells and cortical organoids culture

Human iPSC derived from $CD34^+$ cord blood cells using a three plasmid, seven factors [SOKMNLT; SOX2, OCT4 (POU5F1), Kruppel-like factor (KLF)4, MYC, NANOG, LIN28, and SV40L T antigen] EBNA-based episomal system were purchased free from mycoplasma from Thermo Fisher Scientific (Waltham, MA, cat #A18945). Global gene expression profile of this iPSC line showed that it is indistinguishable from human embryonic stem cells (ESC) (Quintanilla et al., 2014), and that directed differentiation analysis demonstrated its potential to develop into ectodermal, mesodermal and endodermal lineages (Burridge et al., 2011). These cells were cultured on Geltrex human ESC-qualified Reduced Growth Factor Basement Membrane Matrix coated 6 wells plates (2 mL medium/well) or 10 cm dishes (10 mL medium/well) using Essential 8 Flex medium and ROCK inhibitor RevitaCell to reduce cellular apoptosis at 37°C with 5% CO_2. The E8 Flex medium formulation was described by Chen et al., Nat Methods, 2011 and consisted of insulin, selenium, transferrin, L-ascorbic acid, FGF2, and TGFβ (or NODAL) in DMEM/F12 with pH = 7.4 adjusted with $NaHCO_3$. When iPSC reached 85% confluence, they were harvested and passaged using Versene solution. All iPSC culture supplies were obtained from Thermo Fisher Scientific.

iPSC-derived brain cortical organoids were developed according to Dr. Lancaster's protocol with minor modifications described by Ormel PR (Harbuzariu et al., 2019; Lancaster et al., 2013, 2017; Ormel et al., 2018) that allowed the development of innate microglia. Brain organoids were developed using STEMdiff Cerebral organoids kits (Stem Cell Technologies cat #08570 and #08571) as recommended by manufacturer's instructions. After iPSC dissociation using Accutase, $9x10^3$ cells were seeded in each well of 96-well round-bottom low attachment plates in embryoid body medium containing a Rho-kinase (ROCK) inhibitor (Y-27632). After 6 days, the embryoid bodies were cultured in induction medium to guide them towards the neuronal fate until day 13 and then expanded in droplets of Corning (Corning, NY) Reduced Growth Factor Matrigel Matrix (no phenol red) on organoid embedding sheets. The droplets were allowed to solidify at 37°C and were then transferred to 6-well ultralow attachment plates to expand the neuroepithelial tissues. After 4 days of growth in Matrigel, on day 17, the matrix was removed from the organoids by mechanical dissociation, and the organoids were grown in maturation medium on an orbital shaker obtained from Infors HT (Annapolis Junction, MD). Maturation medium changes were performed every 3–4 days for up to 100 days. All supplies for cortical organoids culture were purchased from Stem

Cell Technologies (Cambridge, MA). To account for rigor and reproducibility, three batches of organoids with minimum of 32 organoids per batch were made for each experiment. Mycoplasma testing was performed in iPSCs and brain organoids supernatants every 5 passages using MycoProbe Mycoplasma detection kit (R&D Systems, Minneapolis, MN) and was negative.

METHOD DETAILS

CCK-8 assay for proliferation

The Cell counting kit (CCK-8) obtained from Dojindo Molecular Technologies, Inc. (Rockville, MD), is a convenient and sensitive method for cell proliferation assays. It utilizes a highly water-soluble tetrazolium salt, WST-8, which produces a water-soluble formazan dye upon reduction in the presence of an electron mediator. The amount of the formazan generated from WST-8 reduction by dehydrogenases is directly in proportion to the numbers of living cells. After seeding 10,000 cells/well in Geltrex-coated 96 wells plates, they were allowed to adhere and proliferate for 48 hours until reaching 80% confluence, then HRP2, anti-HRP2/ anti-TLR1/anti-TLR2 antibodies (Fisher Scientific) or NRG1 were added. The already mixed CCK-8 solution was subsequently added to the wells, the plates were placed in the incubator for 30 min-1 hour, then absorbance at 450 nm was read using a microplate reader [CytoFluorTM 2300 plate reader and CytoFluorTM 2300 v. 3A1 software (Millipore Co, Bedford, MA]). The absorbance was plotted to determine cell proliferation.

Apoptosis and necrosis assay

To assess early apoptosis/necrosis longitudinally in iPSC cultured with HRP2/anti-TLR1 or anti-TLR2 antibodies, we used the RealTime-Glo Annexin V Apoptosis and Necrosis Assay obtained from Promega (Madison, WI) following the manufacturer's instructions. Briefly, iPSC's were placed in 96-well low attachment plates, and then Annexin NanoBit substrate, CaCl2, necrosis detection reagent, Annexin V-SmBiT and AnnexinV-LgBiT were added. HRP2-induced apoptosis was measured every hour for 6 hours, then at 24 and 26 hours by using a plate reader [CytoFluorTM 2300 plate reader and CytoFluor 2300 v. 3A1 software (Millipore)] set for chemiluminescence, while necrosis was detected by setting up the plate reader for green fluorescence (excitation 485 nm, emission 525 nm).

Immunohistochemistry and immunofluorescence

Immunofluorescence was used to assess the expression of various markers in formalin-fixed iPSC, while immunohistochemistry was conducted to evaluate the localization of proteins in cortical organoids dehydrated with ethanol and embedded in paraffin blocks.

Immunocytochemical analysis of iPSC

Several days prior to staining, iPSC were passaged to Lab-Tek (Fisher Scientific, Waltham, MA) chamber slides coated with Geltrex, then fixed with 4% paraformaldehyde, blocked with 0.3% Triton X-(for permeabilization) (Sigma, St Louis, MO) and 10% goat serum (Vector Laboratories Inc, Burlingame, CA), the incubated with primary antibody [Ki67(BD Biosciences, San Jose, CA), Sox2 (EMD Millipore, St. Louis, MO), CXCL10 (PeproTech (Rocky Hill, NJ), CXCR3 (Abcam), HRP2 (] overnight. After washing the slides with DPBS, the secondary antibody was added (anti-rabbit secondary conjugated with Cy3 from Sigma, St. Louis, MO and anti-mouse Alexa 488 from Invitrogen, Carlsbad, CA), then Prolong gold anti-fade reagent with DAPI (Invitrogen) was added.

Immunohistochemical analysis of brain cortical organoids

Brain cortical organoids at 20-100 days in culture were fixed with 10% formalin, dehydrated with ethanol, and embedded in paraffin blocks. 10 μm thick sections were deparaffinized with xylene, rehydrated in a graded series of ethanol and double distilled water in a standard manner, and then stained with H&E. To detect protein expression, the sections were heated to unmask the epitopes, blocked with 10% goat serum, then primary antibodies were added overnight [Sox2 from EMD Millipore, β III tubulin (TUJ1, BioLegend, San Diego, CA)]; IBA-1, NRG1, ErbB4, GFAP, CXCR3, Ang2 and Ang1 from Abcam; Brachyury from R&D Systems; Cleaved caspase 3 (CC3), NFL and NFM from Cell Signaling, Danvers, MA; BDNF from Thermo Fisher Scientific and CXCL-10 from PeproTech (Rocky Hill, NJ). Fluorescence staining was performed using fluorochrome-labelled secondary antibodies (Alexa Fluor 488, Alexa Fluor 647, Invitrogen). The sections were covered with Vectashield mounting medium containing DAPI (H-1200) obtained from Vector Laboratories Inc (Burlingame, CA).

Protein expression analysis

Images for both immunocytochemistry and immunohistochemistry were collected using a Zeiss 700 confocal laser scanning microscope (LSM) and a Zeiss 780 Elyra super resolution microscope, while images were captured using Zen black software (Carl Zeiss Microscopy, While Plains, NY). For brightfield imaging, an Olympus microscope (Irvine, CA) was used. We measured the intensity of ERBB4, NRG1, CC3, TUJ1, IBA1, GFAP, BDNF, CXCL10, CXCR3, Ang-2, Ang-1, NFL and NFM staining using ImageJ software. After splitting the channels to obtain the red and green channels, the images were changed to grey scale, and then the fluorescence intensity was measured to determine marker expression. Mean intensity for each measurement was reported to DAPI. At least 3 forebrain structures from 3 separate organoids were analyzed per treatment type. To obtain publication quality photos, we used the same settings on Adobe Lightroom editor to increase their clarity and contrast.

Western blot analysis

To assess the Toll like receptors (TLR) expression and to investigate the apoptosis in cortical organoids treated with HRP2 +/− NRG1, cell lysates were prepared using RIPA buffer (Sigma) containing protease/phosphatase inhibitors (Thermo Fisher Scientific). The protein concentration was determined in each sample using a Pierce BCA Protein Assay Kit (Thermo Fisher Scientific). Thirty to fifty micrograms of total protein from cell lysates were loaded on AnyKD or 4–15% SDS-polyacrylamide gels. After electrophoresis, the proteins were transferred to PVDF membranes using a Trans Blot Turbo Transfer System (BioRad). After blocking for 30 min in 5% skim milk-TBST buffer (TBS plus 0.1% Tween 20), the membranes were incubated with primary antibodies [NFkB and TLR4 from Santa Cruz Biotechnology (Dallas, TX); Caspase 3 and 8 from R&D Systems, PARP and TLR 1, 2, 3, 6, 7, 8, 9 from Cell Signaling; TLR5 from Abcam]. overnight at 4°C. Next, the membranes were incubated with horseradish peroxidase (HRP)-conjugated secondary antibodies and chemiluminescent substrate (Thermo Fisher Scientific). Specific antigen expression was evaluated using an iBright CL1500 Imaging System (Thermo Fisher Scientific). GAPDH or β-actin were used as the experimental protein loading control. The quantitative determination of proteins was performed using ImageJ. We drew a box around each band of interest (with a minimum inclusion of surrounding background) and the housekeeping proteins and measured their intensity. We picked the basal lane as the reference and then calculated the normalization factor for each lane by deriving the percent of the signal of the housekeeping protein in each lane, using the basal lane as the numerator. This percent represents the difference in sample load between the reference and the other lanes of interest (Basal, HRP2 and HRP2+NRG1).

Gene expression analysis

RNA extraction

Cortical organoids grown for 50 days in culture and treated with HRP2+/- NRG1 were collected, and RNA was extracted using PARIS kit (Thermo Fisher Scientific). The organoids were homogenized using disruption reagent, then the lysates were mixed with an equal volume of lysis/binding solution to prevent RNA degradation by cellular ribonucleases. Next, 100% ethanol was added to the lysate, the sample mixture was applied to a filter cartridge and treated with elution solution preheated at 95-100 C, then the RNA was recovered by centrifugation. The RNA concentration was determined by reading the absorption at 260/280 nm using a NanoDrop Spectrophotometer (Thermo Fisher Scientific).

Gene array

To determine the immunology genes that were up-or down-regulated by HRP2 and whether NRG1 reversed these effects, we used the nCounter platform (NanoString, Seattle, WA) that quantified RNA directly using molecular barcode technology. RNA was directly tagged with a capture probe and a reporter probe that are specific for the Human Immunology gene panel with more than 500 target genes, creating a unique target-probe complex. Fold changes and P values were calculated using Student's t-test. A p value <0.05 with a fold change between HRP2 and untreated samples greater than 2.0 were considered to be a significant dysregulation.

Molecular pathway analysis

We identified up- and down-regulated genes that were significantly associated with HRP2 treatment on cortical organoids at 50 days in culture and results were analyzed using nSolver (NanoString) software. Each gene identifier was mapped to its corresponding gene object in the FunRich Database. Organoids treated with HRP2 relative to untreated were overlaid onto global molecular network in the FunRich human

database. Networks of focus genes were generated based on their connectivity and association with biological function and disease most significant for the dataset. Genes are represented by nodes and the biological relationship between them by lines.

QUANTIFICATION AND STATISTICAL ANALYSIS

All experiments and measurements were performed in at least 3 cortical organoids from different batches in three biological replicates. We used GraphPad Prism to make statistical comparisons using Student's t test and one-or two-way ANOVA. Data are presented as the means +/− SEM. Values of $p < 0.05$ were considered statistically significant.